Molecular Cancer Research

RASEF is a novel diagnostic biomarker and a therapeutic target for lung cancer

Hideto Oshita, Ryohei Nishino, Atsushi Takano, et al.

Mol Cancer Res Published OnlineFirst May 16, 2013.

RASEF is a novel diagnostic biomarker and a therapeutic target for lung cancer

Hideto Oshita[1,3], Ryohei Nishino[1], Atsushi Takano[1,2], Takashi Fujitomo[1], Masato Aragaki[1], Tatsuya Kato[1,6], Hirohiko Akiyama,[4] Eiju Tsuchiya,[5] Nobuoki Kohno[3], Yusuke Nakamura[1], Yataro Daigo[1,2*]

[1]Laboratory of Molecular Medicine, Human Genome Center, Institute of Medical Science, The University of Tokyo, Tokyo 108-8639, Japan

[2]Department of Medical Oncology and Cancer Center, Shiga University of Medical Science, Otsu 520-2192, Japan

[3]Department of Molecular and Internal Medicine, Graduate School of Biomedical Sciences, Hiroshima University, Hiroshima 734-8551, Japan

[4]Department of Thoracic Surgery, Saitama Cancer Center, Saitama 362-0806, Japan

[5]Kanagawa Cancer Center Research Institute, Yokohama 241-0815, Japan

[6]Department of Surgical Oncology, Hokkaido University Graduate School of Medicine, Sapporo 060-8638, Japan

*Request for reprints: ydaigo@ims.u-tokyo.ac.jp

Running title: RASEF as a Novel Oncogene

Key words: oncogenes, cancer antigen, biomarker, therapeutic target, lung cancer

Abstract

Genome-wide gene expression profile analyses revealed that Ras and EF-hand domain containing (*RASEF*) was significantly transactivated in the majority of lung cancers. Transient expression of RASEF promoted cell growth, whereas transfection of siRNA for *RASEF* to lung cancer cells reduced its expression and resulted in growth suppression of the cancer cells. Immunohistochemical staining using tumor tissue microarrays consisting of 341 archived non-small cell lung cancers revealed the association of strong RASEF positivity with poor prognosis (P = 0.0034 by multivariate analysis). RASEF could bind to extracellular signal-regulated kinase (ERK) 1/2 and appeared to enhance the ERK1/2 signaling. In addition, inhibition of interaction between RASEF and ERK1/2 using cell-permeable peptide that corresponded to the ERK1/2-interacting site of RASEF protein, suppressed growth of lung cancer cells. RASEF may play important roles in lung carcinogenesis, and could be useful as a prognostic biomarker and a target for the development of new molecular therapies.

Introduction

Lung cancer is the most common cause of cancer-related death in the world and its incidence has been increasing (1). In spite of the use of advanced surgical treatments combined with radiotherapy and chemotherapy, the overall 5-year survival rate of lung cancer patients still remains at 20% (2). Development of molecular targeted drugs such as gefitinib and bevacizumab have improved treatment modalities of lung cancer, but fatal adverse events such as interstitial pneumonia by gefitinib or severe hemorrhage by bevacizumab were reported (3–4). Therefore, further development of new agents targeting cancer-specific molecules with no or minimum risk of adverse effect is urgently awaited. To date, clinical and pathological staging have been the most reliable information for physicians in the choice of therapy. However, considering that about 30% of stage I non-small-cell lung cancer (NSCLC) patients who had undergone curative surgery suffered recurrent diseases (2), it is important to develop more precise prognostic biomarkers for selecting patients who should be treated with adjuvant therapies and intensively followed after surgical treatment.

Systematic analysis of expression levels of thousands of genes using a cDNA microarray technology is an effective approach for identifying molecules involved in pathways of carcinogenesis or those associated with efficacy/resistance to anticancer therapy; some of such genes or their gene products may be good target molecules for the development of novel therapies and/or cancer biomarkers (5). To identify such molecules, particularly oncoantigens, we had performed genome-wide expression profile analysis of 120 clinical lung cancer tissue samples, coupled with enrichment of tumor cells by laser microdissection,

and then compared the expression profile data with those in 31 normal human tissues (27 adult and 4 fetal organs) (6–10). To verify the clinicopathological significance of the respective gene products, we have established a screening system by a combination of the tumor-tissue microarray analysis of clinical lung cancer materials and RNA interference technique (11–41). This systematic approach revealed that RAS and EF-hand domain containing (RASEF) is likely to be a novel molecule that was overexpressed commonly in primary lung cancers and was essential for cell growth and/or survival of cancer cells.

RASEF contains a Rab GTPase domain in the C-terminal region and is considered as a member of Rab GTPase protein family. Unlike other Rab proteins, RASEF contains two EF-hand domains which are generally known to be important for binding to calucium ions in the N-terminus and a coiled-coil motif in an internal region (42). The functional relevance of RASEF activation to carcinogenesis as well as its detailed biological function has not yet been defined. We here report the first evidence that RASEF plays a significant role in lung cancer cell growth possibly through its interaction with extracellular signal-regulated kinase (ERK) 1/2, and suggest that RASEF could be a promising prognostic biomarker and therapeutic target for lung cancer.

Materials and Methods

Cell lines and tissue samples

Lung cancer cell lines and human bronchial epithelial cells (BEAS-2B) used in this study were listed in **Supplementary Table S1**. A427, A549, NCI-H1373, NCI-H1781, NCI-H358, NCI-H226, NCI-H520, NCI-H2170, NCI-H1703, DMS114, DMS273, NCI-H196 NCI-H446, and BEAS-2B cells were from American Type Culture Collection in 2003, 2010 and 2011, and tested and authenticated by DNA profiling for polymorphic short tandem repeat (STR) markers. PC-3, SBC-3 and SBC-5 cells were from Japanese Collection of Research Bioresources (JCRB) in 2001 and 2010, and tested and authenticated by DNA profiling for polymorphic short tandem repeat (STR) markers. PC-14, EBC-1 and RERF-LC-AI cells were from RIKEN BioResource Center in 2001 and 2010, and tested and authenticated by DNA profiling for polymorphic short tandem repeat (STR) markers. LC319 cells were from Aichi Cancer Center in 2003, and tested and authenticated by DNA profiling for single-nucleotide polymorphism, mutation, and deletion analysis. PC-9 and LX1 cells were from Tokyo Medical University and Central Institute for Experimental Animals and European Collection of Animal Cell Cultures in 2002, and tested and authenticated by DNA profiling for single-nucleotide polymorphism, mutation, and deletion analysis. All cells were grown in monolayer in appropriate medium supplemented with 10% FCS and maintained at 37°C in humidified air with 5% CO_2. Primary lung cancer samples had been obtained earlier as previously described (6, 10). All tumors were staged on the basis of the pTNM pathological classification of the UICC (International Union Against Cancer) (43). A total of 341 formalin-fixed samples

of primary NSCLCs (100 female and 241 male patients; median age of 65 with a range of 35-85 years; 93 never smoke cases and 248 ex- or current smokers; 205 adenocarcinomas (ADCs), 105 suqamous cell carcinomas (SCCs), 11 adenosquamous cell carcinoma (ASCs), 20 large cell carcinoma (LCCs); 141 pT1, 157 pT2 and 43 pT3 cases; 223 pN0, 42 pN1, and 76 pN2 cases: see **Supplementary Table S2**) had been obtained earlier along with clinicopathological data from patients undergoing surgery at Saitama Cancer Center (Saitama, Japan). Independent set of 243 formalin-fixed samples of primary NSCLCs for validation study was obtained by Hokkaido University and its affiliated hospitals (Sapporo, Japan). These patients received resection of their primary cancers, and among them only patients with positive lymph node metastasis were treated with cisplatin-based adjuvant chemotherapies after their surgery. This study and the use of all clinical materials mentioned were approved by individual institutional Ethical Committees.

Semi-quantitative reverse transcription-PCR

A total of 3 μg aliquot of mRNA from each sample was reversely transcribed to single-stranded cDNAs using random primer (Roche Diagnostics) and SuperScript II (Invitrogen). Semi-quantitative reverse transcription-PCR (RT-PCR) experiments were carried out with the following sets of synthesized gene-specific primers or with β-actin (*ACTB*)-specific primers as an internal control: *RASEF*, 5'-GGCTGACATTCGTGACACTG-3' and 5'-GGAATTGGTCCCGGTTAGAT-3'; Cyclin D1 (*CCND1*), 5'-CCTCGGTGTCCTACTTCAAA-3' and 5'-CCAGGTTCCACTTGAGCTTGT-3';

Cyclin B1 (*CCNB1*), 5'-TTGGTGTCACTGCCATGTTT-3' and 5'-GATGCTCTCCGAAGGAAGTG-3'; Cyclin-dependent kinase inhibitor 1A (*CDKN1A*), 5'-TTAGCAGCGGAACAAGGAGT-3' and 5'-ATTCAGCATTGTGGGAGGAG-3'; beta-actin (*ACTB*), 5'-GAGGTGATAGCATTGCTTTCG-3' and 5'-CAAGTCAGTGTACAGGTAAGC-3'. PCRs were optimized for the number of cycles to ensure product intensity to be within the linear phase of amplification.

Western blot analysis

Cell lysates from lung cancer cell line or normal airway epithelial cells were subjected to Western blotting. In brief, cells were incubated in 1 mL lysis buffer (0.5% NP-40, 50mmol/L Tris-HCl, 150mmol NaCl) in the presense of protease inhibitor (Protease Inhibitor Cocktail Set III; Calbiochem). Western blotting were done using an ECL Western-blotting analysis system (GE Healthcare Bio-sciences) as described previously (11-15). A commercially available rabbit polyclonal antibody to human RASEF (Catalog No. 11569-1-AP, Proteintech Group, Inc.) was confirmed to be specific to endogenous RASEF protein by Western-blot analysis using lysates of lung cancer cell lines as well as normal airway epithelial cells (negative control).

Immunocytochemical analysis

Cells were plated onto glass coverslips (Becton Dickinson Labware), fixed with 4% paraformaldehyde, and permeabilized with 0.1% Triton X-100 in PBS for 3

min at room temperature. Nonspecific binding was blocked by Casblock (ZYMED) for 10 min at room temperature. Cells were then incubated for overnight at 4°C with a rabbit polyclonal antibody to RASEF (Catalog No. 11569-1-AP, Proteintech Group, Inc.) diluted in PBS containing 1% BSA. After being washed with PBS, the cells were stained by Alexa 488-conjugated secondary antibody (Invitrogen) for 60 min at room temperature. After another wash with PBS, each specimen was mounted with Vectashield (Vector Laboratories, Inc.) containing 4',6-diamidino-2-phenylindole (DAPI) and visualized with Spectral Confocal Scanning Systems (TSC SP2 AOBS; Leica Microsystems).

Northern blot analysis

Human multiple tissue blots covering 16 tissues (BD Biosciences) were hybridized with an [α-^{32}P]-dCTP-labeled, 421-bp PCR product of *RASEF* that was prepared as a probe using primers 5'-GGCTGACATTCGTGACACTG-3' and 5'-CAAAGTTCCAGAGGGACCTG-3'. Prehybridization, hybridization, and washing were done following the manufacturer's specifications. The blots were autoradiographed with intensifying screens at -80°C for 10 days.

Immunohistochemistry and tissue microarray

To investigate the clinicopathological significance of RASEF overexpression in lung cancers, we stained tissue sections using ENVISION+ Kit/HRP (DakoCytomation). Anti-RASEF rabbit polyclonal antibody (Catalog No. 11569-1-AP, Proteintech Group, Inc.) was added after blocking of endogenous

peroxidase and proteins, and each section was incubated with HRP-labeled anti-rabbit IgG as the secondary antibody. Substrate-chromogen was added and the specimens were counterstained with hematoxylin.

Tumor tissue microarrays were constructed with formalin-fixed 341 primary lung cancers, each of which had been obtained with an identical protocol to collect, fix, and preserve the tissues after resection (12-18). The tissue area for sampling was selected based on visual alignment with the corresponding H&E-stained section on a slide. Three, four, or five tissue cores (diameter, 0.6 mm; depth, 3–4 mm) taken from a donor tumor block were placed into a recipient paraffin block with a tissue microarrayer (Beecher Instruments). A core of normal tissue was punched from each case, and 5-μm sections of the resulting microarray block were used for immunohistochemical analysis. Three independent investigators semi-quantitatively assessed RASEF positivity without prior knowledge of clinicopathologic information. The intensity of RASEF staining was evaluated using the following criteria: strong positive (scored as 2+), brown staining in > 50% of tumor cells completely obscuring cytoplasm; weak positive (1+), any lesser degree of brown staining appreciable in tumor cell cytoplasm; and absent (scored as 0), no appreciable staining in tumor cells. Cases were accepted as strongly positive only if two or more investigators independently defined them as such.

Statistical analysis

Statistical analyses were done using the StatView statistical program (SAS). Tumor-specific survival curves were calculated from the date of surgery to the

time of death related to NSCLC or to the last follow-up observation. Kaplan-Meier curves were calculated for each relevant variable and for RASEF expression; differences in survival times among patient subgroups were analyzed using the log-rank test. Univariate and multivariate analyses were done with the Cox proportional hazard regression model to determine associations between clinicopathological variables and cancer-related mortality. First, we analyzed associations between death and possible prognostic factors, including age, gender, smoking status, pathologic tumor classification, and pathologic node classification, taking into consideration one factor at a time. Second, multivariate Cox analysis was applied on backward (stepwise) procedures that always forced strong RASEF expression into the model, along with any and all variables that satisfied an entry level of a *P* value of < 0.05. As the model continued to add factors, independent factors did not exceed an exit level of $P < 0.05$.

RNA interference assay

To evaluate the biological functions of RASEF in lung cancer cells, we used small interfering RNA (siRNA) duplexes against RASEF. The target sequences of the synthetic oligonucleotides for RNA interference were as follows: control 1 (*EGFP*: enhanced green fluorescent protein (GFP) gene, a mutant of *Aequorea victoria* GFP), 5'-GAAGCAGCACGACUUCUUC-3'; control 2 (*LUC*: luciferase gene from *Photinus pyralis*), 5'-CGTACGCGGAATACTTCGA-3'; siRNA-RASEF-#1, 5'-GTTAGTACCTTGTACCAAA-3'; siRNA-RASEF-#2, 5'-CTTCATCCGTGAGATCAGA-3'. siRNAs were transfected into lung cancer

cell lines, A549 and NCI-H2170 using 30 μL of Lipofectamine 2000 (Invitrogen) following the manufacturer's protocol. Cell numbers and viability were measured by Giemsa staining and triplicate MTT assays (cell counting kit-8 solution; Dojindo Laboratories) at 5 days after the transfection. Expression of endogenous RASEF protein was detected by Western blotting.

Cell growth assays

Endogenous RASEF-negative BEAS-2B and DMS114 cells transfected either with RASEF expression vector (pCAGGSn3FH-RASEF), which express RASEF with 3 X Flag sequences (DYKDHDGDYKDHDIDYKDDDDK) at the NH_2-terminal or with mock vector (pCAGGSn3FH) were seeded onto six-well plates (5 X 10^4 cells/well), and maintained in medium containing 10% FBS and geneticin. After 120 hours, cell proliferation was evaluated by the MTT assay using Cell Counting Kits (Dojindo Laboratories).

Immunoprecipitation assay

To examine the interaction between endogenous RASEF and ERK1/2, immunoprecipitation was performed with a rabbit polyclonal anti-RASEF antibody (Catalog No. 11569-1-AP, Proteintech Group, Inc.) at 4°C for 2 hours after incubation of extracts from NCI-H2170 cells at 4°C for 1 hour with protein G-Agarose beads as described previously (14). The immunoprecipitates were washed five times with lysis buffer, and were subjected to Western blotting with a mouse monoclonal anti-ERK1/2 antibody (Catalog. No. 4696; Cell Signaling Technology).

Identification of ERK1/2-interacting sites on RASEF

To define the ERK1/2-interacting sites on RASEF protein, we constructed various vectors expressing partial RASEF protein with Flag-tag at its N-terminus, and transfected either of them into RASEF-negative DMS114 cells. Immunoprecipitation using anti-Flag M2 agarose and subsequent immunoblotting with anti-ERK1/2 antibody were performed as described above.

Synthesized dominant-negative peptide

To further investigate the biological importance of the interaction between RASEF and ERK1/2 that had been confirmed by above mentioned assays in lung cancer cell growth, the three different 23-amino-acid polypeptides covering the ERK1/2-interacting site on RASEF 520-575 with a membrane-permeable 11 residues of arginine (11R) at its N-terminus (11R-RASEF 520-542, RRRRRRRRRRR-GGG-SALSPQTDLVDDNAKSFSSQKAY; 11R-RASEF 536-558, RRRRRRRRRRR-GGG-FSSQKAYKIVLAGDAAVGKSSFL; 11R-RASEF 553-575, RRRRRRRRRRR-GGG-GKSSFLMRLCKNEFRENISATLG) were synthesized as previously described (17, 20, 28, 29). Scramble peptides (SCR) derived from the 11R-RASEF 553-575 peptides that showed growth suppressive effect on cancer cells were synthesized as a control (RRRRRRRRRRR-GGG-RSENKMSLFRGSEFTLLKGCINA). Peptides were purified by preparative reverse-phase high-performance liquid chromatography with the purity of >95%. Two RASEF-positive cell lines A549 and NCI-H2170,

and RASEF-negative bronchial epithelial cells BEAS-2B were cultured in the presence of either of these peptides in media at the concentration of 5, 10, or 15 μM for 5 days. The medium was replaced at every 48 hours with the above-mentioned concentrations of each peptide, and the viability of cells was evaluated by MTT assay.

Results

RASEF expression in lung cancers and normal tissues

To identify novel molecules that can be applicable for the development of novel biomarkers and treatments on the basis of the biological characteristics of cancer cells, we had performed genome-wide gene expression profile analysis of 120 lung carcinomas using a cDNA microarray (6–10). Among 27,648 genes or expressed sequence tags screened, we identified elevated expression (5-fold or higher) of *RASEF* transcript in the great majority of the lung cancer samples examined. We confirmed by semi-quantitative RT-PCR experiments *RASEF* expression in 9 of 12 clinical lung cancers, but its expression was hardly detectable in their corresponding normal lung tissues (**Fig. 1*A***). We also observed overexpression of *RASEF* in 14 of 22 lung cancer cell lines, but did not detect its expression in BEAS-2B airway epithelial cells (**Fig. 1*B***). To evaluate the expression levels and subcellular localization of RASEF protein in lung cancer cells, we performed Western blotting and immunofluorescence analyses using a rabbit anti-RASEF polyclonal antibody and *RASEF*-positive lung cancer A549 and NCI-H2170 cells, and *RASEF*-negative DMS114 cells as well as BEAS-2B airway epithelial cells. The band was detected by Western blotting at

the molecular weight of about 90kD in *RASEF*-positive A549 and NCI-H2170 cells, whereas no signal was detected in *RASEF*-negative DMS114 and BEAS-2B cells (**Fig. 1*C***). Since there are several predicted phosphorylation sites on RASEF, we treated the lysate of NCI-H2170 cells with phosphatase, and observed by immunoblotting the disappearance of the upper weak signals, suggesting the phosphorylation of a part of RASEF protein in cancer cells (**Supplementary Fig. S1**). We also detected by immunofluorescence analysis RASEF protein mainly in the cytoplasm of *RASEF*-positive A549 and NCI-H2170 cells, but not in *RASEF*-negative DMS114 and BEAS-2B cells (**Fig. 1*D***).

Northern blot analysis using a *RASEF* cDNA fragment as a probe identified a 5.8-kb transcript only in prostate and testis, but not in any other normal tissues examined (**Fig. 2*A***). We also examined by immunohistochemical analysis expression of RASEF protein in six normal human tissues (liver, heart, kidney, lung, prostate, and testis) and lung cancer tissues (ADC, SCC, and SCLC). Strong positive RASEF staining was mainly observed in cytoplasm of lung tumor cells, and weakly in prostate and testicular cells, but its staining was hardly detectable in the remaining four normal tissues (**Fig. 2*B***). The comparison of RASEF staining in NSCLC and adjacent normal tissues from 10 patients who underwent surgery revealed that RASEF protein was highly expressed in NSCLC tissues, but not in adjacent normal lung tissues (**Fig. 2*C***).

Association of RASEF expression with poor prognosis for NSCLC patients

To investigate the biological and clinicopathological significance of RASEF in

pulmonary carcinogenesis, we carried out immunohistochemical staining on tissue microarray containing 341 NSCLC cases that underwent surgical resection, using a rabbit polyclonal antibody specific to RASEF. We classified a pattern of RASEF expression on the tissue array ranging from absent (scored as 0) to weak/strong positive (scored as 1+ to 2+; representative images of staining were shown in **Fig. 2*D***). Of the 341 NSCLCs, RASEF was strongly stained in 126 (37%) cases (score 2+), weakly stained in 150 (44%) cases (score 1+), and not stained in 65 (19%) cases (score 0) (**Table 1*A***). Using the scores of RASEF staining, we examined the association between RASEF positivity and prognosis of NSCLC patients, and found that the prognosis of NSCLC was likely to be poorer in patients with the higher scores of RASEF positivity than those with the lower scores, although there is no significant difference of survival periods between NSCLC patients with weak RASEF-positive tumors and those with RASEF-negative (**Supplementary Fig. S2**). Therefore we next examined correlation of RASEF expression (strong positive vs weak positive/absent) with prognosis of patients as well as various clinicopathologic parameters such as age, gender, smoking status (never smoker vs current or former smoker), pathologic tumor stage (tumor size; T1 vs T2-3), pathologic node stage (node status; N0 vs N1-2), and histology (ADC vs other histological types), and found that strong RASEF positivity was associated with poor prognosis of patients with NSCLC after the resection of primary tumors ($P < 0.0001$ log-rank test; **Fig. 2*E***). In addition, we found that high levels of RASEF expression were significantly correlated with tumor size (T factor; $P=0.0006$, **Table 1*A***). Furthermore, we applied univariate analysis to evaluate

associations between patient prognosis and several factors including age, gender, smoking status, pathologic tumor stage, pathologic node stage, histology, and RASEF status (score 0, 1+ vs score 2+). All those variables except smoking status were significantly associated with poor prognosis. Multivariate analysis using a Cox proportional hazard model indicated that RASEF (P = 0.0034) as well as other three factors (age, tumor size, and lymph node metastasis) were independent prognostic factors for surgically treated NSCLC patients (**Table 1*B***). To further confirm the independent prognostic value of strong RASEF expression, we performed subgroup analysis of stage I NSCLCs by log-rank test, and found that strong RASEF positivity was associated with poor prognosis of patients with stage I NSCLC (P = 0.0004). We also confirmed prognostic value of RASEF in another independent set of 243 postoperative NSCLC patients (P = 0.0382 log-rank test; **Supplementary Fig. S3**).

Growth effect of RASEF protein

To disclose the role of RASEF in the growth or survival of cancer cells, we suppressed endogenous RASEF expression using two siRNAs against RASEF (si-RASEF-#1 and -#2), along with two control siRNAs (siRNAs for *EGFP* and *LUC*). Transfection of si-RASEFs into lung cancer cells decreased the level of RASEF protein, and resulted in significant reduction of cell viability and colony numbers measured (**Figs. 3*A*-*C***; statistical analysis of colony formation assay is in **Supplementary Fig. S4**). These results suggest that RASEF is indispensable for cell growth or survival of lung cancer cells.

We further evaluated the role of RASEF in cell growth by introducing RASEF expression vector or mock plasmid into BEAS-2B bronchial epithelial cells and DMS114 lung cancer cells, which scarcely expressed endogenous RASEF. We observed significantly rapid growth of the cells transfected with RASEF expression vector compared with those with mock plasmid (**Figs. 3*D* and 3*E***). These data further imply RASEF to be important for growth of cells.

Elevation of phosphorylated ERK1/2 by RASEF expression

Since it has been reported that some Rab proteins were involved in the positive regulation of Mitogen-activated protein kinase (MAPK) cascade that is well-known to be crucial for cell proliferation (44, 45), we subsequently examined the possibility that RASEF could affect the activity of MAPK cascade in lung cancer cells. We first investigated by Western blot analysis of lung cancer cells the phosphorylation levels of three MAPK molecules, c-Raf, MEK1/2, and ERK1/2 according to the levels of RASEF introduction or reduction. Transfection of RASEF-expression vector into endogenous RASEF-negative DMS114 cells increased the levels of phospho-ERK1/2 (pERK1/2) compared with that of mock vector, whereas the levels of total ERK1/2 protein were not different between the cells transfed with RASEF-expression vector and those with mock vector (**Fig. 4*A***). In addition, transfection of siRNAs for RASEF into endogenous RASEF-positive NCI-H2170 cells suppressed RASEF expression, and resulted in significant decrease of the phosphorylated ERK1/2 (pERK1/2), but not total ERK1/2 (**Fig. 4*B***). The levels of pMEK1/2 and pc-Raf as well as total MEK1/2 and total c-Raf, which are upstream kinases of ERK1/2

were not changed in these two assays (**Figs. 4*A* and 4*B***), suggesting that RASEF protein expression could selectively enhance ERK1/2 phosphorylation. Moreover, transfection of RASEF-expression vector into RASEF-negative DMS114 cells increased the phosphorylation levels of RSK (pRSK (T359/S363)), but did not affect the levels of total RSK which is one of the substrate of ERK1/2 kinase, while inhibition of RASEF protein expression by siRNAs for RASEF in RASEF-positive NCI-H2170 cells reduced the levels of pRSK (T359/S363), but not those of total RSK, implying that RASEF protein expression could activate downstream cascade of ERK1/2 such as RSK (**Figs. 4*A* and 4*B***).

We also evaluated by semi-quantitative RT-PCR the expression levels of *CCND1 CCNB1*, and *CDKN1A* which were known to be transcriptionally up- or down-regulated by MAPK pathway (46, 47). *CCND1* and *CCNB1* are reported to be transactivated by activation of MAPK pathway, while *CDKN1A* is negatively regulated. As expected, overexpression of RASEF protein in RASEF-negative BEAS-2B and DMS114 cells increased the expression of both *CCND1* and *CCNB1*, and reduced that of *CDKN1A* (**Fig. 4*C***). On the other hand, suppression of RASEF protein expression by siRNAs in RASEF-positive A549 and NCI-H2170 cells reduced the expression of both *CCND1* and *CCNB1*, and increased *CDKN1A* expression (**Fig. 4*D***). These results indicate that presence of RASEF protein might activate ERK1/2 signaling pathway in lung cancer cells.

Since cell-based assays suggested that the presence of total RASEF protein in lung cancer cells could elevate the levels of phospho-ERK1/2, but not those of total ERK1/2 protein, we subsequently evaluated the association between total RASEF protein expression and the levels of phospho-ERK1/2 in 8 lung cancer

cell lines and BEAS-2B cells (**Supplementary Fig. S5*A***). The Spearman correlation coefficient indicated that relative ERK1/2 phosphorylation, which was defined as phospho-ERK signal / total ERK protein signal, was significantly correlated with expression levels of total RASEF protein (**Supplementary Fig. S5*B***), suggesting that presence of total RASEF protein could increase the levels of phospho-ERK1/2.

We further carried out immunohistochemical staining on tissue microarray of 323 NSCLCs using a rabbit anti-phospho-ERK1/2 (pERK1/2) polyclonal antibody, and compared its expression with total RASEF protein positivity, which were classified as strong positive, weak positive or absent staining. We confirmed that strong total RASEF protein positivity was significantly correlated with strong phospho-ERK1/2 positivity using chi-square test (χ^2 = 16.778, P < 0.0001; representative images were shown in **Supplementary Fig. S6**).

Identification of ERK1/2-interacting sites on RASEF

To investigate the molecular biological mechanism of regulation of ERK1/2 phosphorylation by total RASEF protein, we examined the interaction between endogenous RASEF and ERK1/2 by immunoprecipitation assay using extracts from lung cancer NCI-H2170 cells and anti-RASEF antibody, and detected binding of endogenous RASEF to endogenous ERK1/2 (**Fig. 5*A***), suggesting that phosphorylation of ERK1/2 was likely to be increased through its interaction with RASEF. The results support the hypothesis that total RASEF protein expression might play important role in a subset of clinical lung cancers probably through its interaction with and subsequent enhancement of the phosphorylation

levels of ERK1/2.

To narrow down the ERK1/2-interacting sites on RASEF, we first constructed 3 vectors expressing partial RASEF protein with Flag-tag ($RASEF_{1-240}$, $RASEF_{170-520}$, and $RASEF_{455-740}$; **Fig. 5*B***) and transfected either of them into DMS114 cells. Immunoprecipitation assay indicated that the only COOH-terminal portion of RASEF ($RASEF_{455-740}$) including a RAB domain was able to bind to endogenous ERK1/2 (**Fig. 5*C***). To further define the minimal ERK1/2-interacting sites, we constructed 4 additional vectors expressing 55-amino-acid protein derived from a COOH-terminal portion of RASEF ($RASEF_{520-575}$, $RASEF_{575-630}$, $RASEF_{630-685}$ and $RASEF_{685-740}$; **Fig. 5*A***) and transfected either of them into DMS114 cells. Immunoprecipitation assay with anti-Flag M2 agarose and subsequent Western blotting with anti-ERK1/2 antibody revealed that $RASEF_{520-575}$ was able to bind to ERK1/2, but other peptides were not (**Fig. 5*D***). These experiments indicate that the 55-amino-acid polypeptide in RASEF (codons 520-575) should be responsible for the interacting to ERK1/2.

Growth inhibition of lung cancer cells by dominant-negative peptides inhibiting RASEF-ERK1/2 interaction

To examine whether RASEF-ERK1/2 interaction could be essential for cancer cell growth, we synthesized three different kinds of 23-amino acid polypeptides covering the ERK1/2-interacting site on RASEF at codons 520-575 with membrane-permeable 11 residues of arginine (11R) at its N-terminus (11R-$RASEF_{520-542}$, 11R-$RASEF_{536-558}$, and 11R-$RASEF_{553-575}$) (**Fig. 6*A***).

Initially, we evaluated the effect of inhibition of the RASEF-ERK1/2 interaction on lung cancer cell growth, we incubated RASEF-positive A549 and NCI-H2170 cells, and RASEF-negative BEAS-2B cells with each of the three peptides at the final concentration of 5, 10, or 15 μM in culture media. MTT assay revealed that the only 11R-RASEF$_{553\text{-}575}$ peptide showed growth suppressive effect on A549 and NCI-H2170 cells on a dose-dependent manner, but not on BEAS-2B cells (**Figs. 6*B* and 6*C***). We also confirmed by immunoprecipitation assay using antibodies to RASEF and ERK1/2 that the endogenous RASEF-ERK1/2 binding was inhibited by addition of 11R-RASEF$_{553\text{-}575}$ peptides, but not its control scramble peptides into culture media of lung cancer NCI-H2170 cells (**Fig. 6*D***). The results suggest that RASEF-ERK1/2 interaction plays a critical role in lung cancer cell growth.

Discussion

Recent accumulation of knowledge in cancer genomics introduced new strategies for cancer treatment such as molecular-targeted therapy (5). Molecular targeted drugs are expected to be highly specific to malignant cells, with minimal adverse effects due to their well-defined mechanisms of action. To find such molecules, we established an effective screening system to identify proteins that were activated specifically in lung cancer cells. The strategy was as follows: (a) identification of up-regulated genes in 120 lung cancer samples through the genome-wide gene expression profiles analysis, covering 27,648 genes or ESTs, coupled with laser microdissection; (b) verification of very low or absent expression of genes in normal organs by cDNA microarray analysis and

multiple-tissue Northern blot analysis; (c) confirmation of the clinicopathologic significance of their overexpression using tissue microarray consisting of hundreds of NSCLC tissue samples; and (d) verification of the targeted genes whether they are essential for the survival or growth of lung cancer cells by siRNA. Through this screening system, we have found that RASEF is overexpressed commonly in clinical lung cancer samples and cell lines, and its gene product plays an important role in the growth of lung cancer cells.

RASEF is described as a member of Rab GTPase family which generally plays important roles in vesicle trafficking. To date, a few studies indicated aberrant expression of *RASEF* in human cancers, but results were contradictory; RASEF was reported to be down-regulated in uveal melanomas, whereas it was overexpressed in esophageal squamous cell carcinomas (48, 49). To examine the mechanism of RASEF activation and overexpression in lung cancer, we checked previous publications and databases for *RASEF* including the data of CGH and genome sequencing (http://cancer.sanger.ac.uk/cosmic/gene/). However, missense mutation was indicated in 10 of 904 (1.1%) lung cancers, but no amplification or translocation of *RASEF* gene was reported in lung cancers. Therefore, we speculate that overexpression of RASEF may be mainly caused by epigenetic mechanism. Further analysis of RASEF including screening of activating mutation by functional assays and/or mechanism of epigenetic regulation of RASEF might further clarify the oncogenic function of RASEF.

In this study, we confirmed that inhibition of expression of endogenous RASEF by siRNA resulted in marked reduction of cell viability of lung cancer cells, and that exogenously-introduced RASEF promoted cell growth. Moreover, tissue

microarray analysis using two independent sample sets revealed that strong RASEF expression was a prognostic factor for surgically-treated NSCLC patients. Interestingly, several openly available microarray databases also independently support our data that the higher expression of RASEF is likely to associate with the poorer prognosis of lung cancer patients (PrognoScan; http://www.prognoscan.org/). The data suggest that RASEF contributes to viability and malignant potential of lung cancer cells and should be a clinically promising prognostic biomarker and novel molecule target for this disease.

Several Rab proteins have been reported to activate the MAPK cascade that is an important intracellular signaling pathway for cell proliferation, cell survival, development, cell cycle, angiogenesis, and cell migration. Rab11 regulates JNK pathway as well as typical MAPK cascade during *Drosophila* wing development (44), whereas RBEL1 (Rab-like protein 1) is thought to promote cell growth through activation of ERK signaling in breast cancer cells (45). We examined whether presence of total RASEF protein could affect the activity of MAPK signal molecules by transfection of siRNAs for RASEF or RASEF-expression vectors into lung cancer cells, and found that presence of total RASEF protein could elevate the levels of phospho-ERK1/2, but not the amount of total ERK1/2 protein in lung cancer cells probably through its interaction with total ERK1/2.

Somatic EGFR mutation was reported to be biologically important for the clinical response of NSCLCs to EGFR tyrosine kinase inhibitors such as gefitinib or erlotinib (3, 5). To examine the relevance of strong RASEF expression to this type of NSCLCs with EGFR mutation, we examined the association between

RASEF overexpression and EGFR mutation status in NSCLC tissues (325 cases available) by using specific antibodies to E746-A750 deletion and those to a point mutation (L858R) in EGFR, and found that there was no exclusive or inclusive relationship between strong RASEF expression and EGFR mutation status, although the frequency of EGFR mutation was higher in NSCLCs with strong RASEF positive compared to those with RASEF weak positive or negative (44% vs 25%, P = 0.0012, Chi-square test). RASEF may play an essential role in various types of lung cancer including those with other driver mutations.

Since inhibition of interaction between RASEF and ERK1/2 by RASEF-derived peptides with a membrane-permeable 11 residues of arginine (11R) at its N-terminus inhibited the growth of RASEF-positive lung cancer cells, targeting RASEF-ERK1/2 interaction as well as RASEF itself by small molecules and/or nucleic acid drugs is one of the possible therapeutic approaches for cancer. The MAPK cascade is well characterized to play a critical role in human carcinogenesis, and has been the subject of intense research for discovery of novel anticancer drugs. Selumetinib (AZD6244, ARRY-142886), a selective inhibitor of mitogen-activated protein kinase kinase 1/2 (MEK1/2), was reported to be effective for a subset of cancer patients in clinical trials, but adverse reactions are also observed in a certain portion of the patients (50). Therefore, targeting therapy against cancer-specific co-activator or mediator of MAPK cascade, which is expressed specifically in cancer tissues, but not in normal tissues, should be an alternative approach for cancer treatment with less adverse events. Although the function of RASEF in carcinogenesis remains

unclear, therapeutic strategy targeting RASEF and/or RASEF-ERK1/2 interaction is thought to have a great potential.

Grant Support: This work was supported in part by Grant-in-Aid for Scientific Research (B) and Grant-in-Aid for Scientific Research on Innovative Areas from The Japan Society for the Promotion of Science. Y.D. is a member of Shiga Cancer Treatment Project supported by Shiga Prefecture (Japan).

References

1. Jemal A, Siegel R, Xu J, Ward E. Cancer statistics, 2010. CA Cancer J Clin 2010;60:277–300.
2. Naruke T, Tsuchiya R, Kondo H, Asamura H. Prognosis and survival after resection for bronchogenic carcinoma based on the 1997 TNM staging classification: the Japanese experience. Ann Thorac Surg 2001;71:1759–64.
3. Inoue A, Saijo Y, Maemondo M, Gomi K, Tokue Y, Kimura Y, et al. Severe acute interstitial pneumonia and gefitinib. Lancet 2003;361:137–9.
4. Johnson DH, Fehrenbacher L, Novotny WF, Herbst RS, Nemunaitis JJ, Jablons DM, et al. Randomized phase II trial comparing bevacizumab plus carboplatin and paclitaxel with carboplatin and paclitaxel alone in previously untreated locally advanced or metastatic non-small-cell lung cancer. J Clin Oncol 2004;22:2184–91.
5. Daigo Y, Nakamura Y. From cancer genomics to thoracic oncology: Discovery of new biomarkers and therapeutic targets for lung and esophageal carcinoma. Gen Thorac Cardiovasc Surg 2008;56:43–53.
6. Kikuchi T, Daigo Y, Katagiri T, Tsunoda T, Okada K, Kakiuchi S, et al. Expression profiles of non-small cell lung cancers on cDNA microarrays: identification of genes for prediction of lymph-node metastasis and sensitivity to anti-cancer drugs. Oncogene 2003;22:2192–205.
7. Kakiuchi S, Daigo Y, Tsunoda T, Yano S, Sone S, Nakamura Y. Genome-wide analysis of organ-preferential metastasis of human small cell lung cancer in mice. Mol Cancer Res 2003;1:485–99.
8. Kakiuchi S, Daigo Y, Ishikawa N, Furukawa C, Tsunoda T, Yano S, et al. Prediction of sensitivity of advanced non-small cell lung cancers to gefitinib (Iressa, ZD1839). Hum Mol Genet 2004;13:3029–43.
9. Kikuchi T, Daigo Y, Ishikawa N, Katagiri T, Tsunoda T, Yoshida S, et al. Expression profiles of metastatic brain tumor from lung adenocarcinomas on cDNA microarray. Int J Oncol 2006; 28:799–805.
10. Taniwaki M, Daigo Y, Ishikawa N, Takano A, Tsunoda T, Yasui W, et al. Gene Expression Profiles of Small-Cell Lung Cancers: Molecular Signatures of Lung Cancer. Int J Oncol 2006;29:567–75.
11. Suzuki C, Daigo Y, Kikuchi T, Katagiri T, Nakamura Y. Identification of COX17 as a therapeutic target for non-small cell lung cancer. Cancer Res 2003; 63:7038–41.
12. Kato T, Daigo Y, Hayama S, Ishikawa N, Yamabuki T, Ito T, et al. A novel human tRNA-dihydrouridine synthase involved in pulmonary carcinogenesis. Cancer Res 2005;65:5638–46.
13. Furukawa C, Daigo Y, Ishikawa N, Kato T, Ito T, Tsuchiya E, et al. Plakophilin 3 oncogene as prognostic marker and therapeutic target for lung cancer. Cancer Res 2005; 65:7102–10.
14. Suzuki C, Daigo Y, Ishikawa N, Kato T, Hayama S, Ito T, et al. ANLN plays a critical role in human lung carcinogenesis through the activation of RHOA and by involvement in the phosphoinositide 3-kinase/AKT pathway. Cancer Res 2005;65:11314–25.

15. Ishikawa N, Daigo Y, Takano A, Taniwaki M, Kato T, Tanaka S, et al. Characterization of SEZ6L2 cell-surface protein as a novel prognostic marker for lung cancer. Cancer Sci 2006; 97:737–45.
16. Takahashi K, Furukawa C, Takano A, Ishikawa N, Kato T, Hayama S, et al. The neuromedin u-growth hormone secretagogue receptor 1b/neurotensin receptor 1 oncogenic signaling pathway as a therapeutic target for lung cancer. Cancer Res 2006; 66:9408–19.
17. Hayama S, Daigo Y, Kato T, Ishikawa N, Yamabuki T, Miyamoto M, et al. Activation of CDCA1-KNTC2, members of centromere protein complex, involved in pulmonary carcinogenesis. Cancer Res 2006; 66:10339–48.
18. Kato T, Hayama S, Yamabuki T, Ishikawa N, Miyamoto M, Ito T, et al. Increased expression of IGF-II mRNA-binding protein 1 is associated with the tumor progression in patients with lung cancer. Clin Cancer Res 2007; 13:434–42.
19. Suzuki C, Takahashi K, Hayama S, Ishikawa N, Kato T, Ito T, et al. Identification of Myc-associated protein with JmjC domain as a novel therapeutic target oncogene for lung cancer. Mol Cancer Ther 2007; 6:542–51.
20. Hayama S, Daigo Y, Yamabuki T, Hirata D, Kato T, Miyamoto M, et al. Phosphorylation and activation of cell division cycle associated 8 by aurora kinase B plays a significant role in human lung carcinogenesis. Cancer Res 2007; 67:4113–22.
21. Taniwaki M, Takano A, Ishikawa N, Yasui W, Inai K, Nishimura H, et al. Activation of KIF4A as a Prognostic Biomarker and Therapeutic Target for Lung Cancer. Clin Cancer Res 2007; 13:6624–31.
22. Mano Y, Takahashi K, Ishikawa N, Takano A, Yasui W, Inai K, et al. Fibroblast growth factor receptor 1 oncogene partner as a novel prognostic biomarker and therapeutic target for lung cancer. Cancer Sci 2007; 98:1902–13.
23. Kato T, Sato N, Hayama S, Yamabuki T, Ito T, Miyamoto M, et al. Activation of holliday junction recognizing protein involved in the chromosomal stability and immortality of cancer cells. Cancer Res 2007; 67:8544–53.
24. Kato T, Sato N, Takano A, Miyamoto M, Nishimura H, Tsuchiya E, et al. Activation of Placenta Specific Transcription Factor Distal-less Homeobox 5 Predicts Clinical Outcome in Primary Lung Cancer Patients. Clin Cancer Res 2008; 14:2363–70.
25. Dunleavy EM, Roche D, Tagami H, Lacoste N, Ray-Gallet D, Nakamura Y, et al. HJURP is a Cell-Cycle-Dependent Maintenance and Deposition Factor of CENP-A at Centromeres. Cell 2009; 137:485–97.
26. Hirata D, Yamabuki T, Miki D, Ito T, Tsuchiya E, Fujita M, et al. Involvement of Epithelial Cell Transforming Sequence 2 (ECT2) Oncoantigen in Lung and Esophageal Cancer Progression. Clin Cancer Res 2009; 15:256–66.
27. Sato N, Koinuma J, Fujita M, Hosokawa M, Ito T, Tsuchiya E, et al. Activation of WD repeat and high-mobility group box DNA binding protein 1 in pulmonary and esophageal carcinogenesis. Clin Cancer Res 2010; 16: 226–39.
28. Sato N, Koinuma J, Ito T, Tsuchiya E, Kondo S, Nakamura Y, et al.

Activation of an oncogenic TBC1D7 (TBC1 domain family, member 7) protein in pulmonary carcinogenesis. Genes Chromosomes Cancer 2010; 49: 353–67.
29. Nguyen MH, Koinuma J, Ueda K, Ito T, Tsuchiya E, Nakamura Y, et al. Phosphorylation and activation of cell division cycle associated 5 by mitogen-activated protein kinase play a crucial role in human lung carcinogenesis. Cancer Res 2010; 70: 5337–47.
30. Ishikawa N, Daigo Y, Yasui W, Inai K, Nishimura H, Tsuchiya E, et al. ADAM8 as a novel serological and histochemical marker for lung cancer. Clin Cancer Res 2004; 10:8363–70.
31. Ishikawa N, Daigo Y, Takano A, Taniwaki M, Kato T, Hayama S, et al. Increases of amphiregulin and transforming growth factor-alpha in serum as predictors of poor response to gefitinib among patients with advanced non-small cell lung cancers. Cancer Res 2005; 65:9176–84.
32. Yamabuki T, Takano A, Hayama S, Ishikawa N, Kato T, Miyamoto M, et al. Dickkopf-1 as a novel serologic and prognostic biomarker for lung and esophageal carcinomas. Cancer Res 2007; 67:2517–25.
33. Ishikawa N, Takano A, Yasui W, Inai K, Nishimura H, Ito H, et al. Cancer-testis antigen lymphocyte antigen 6 complex locus K is a serologic biomarker and a therapeutic target for lung and esophageal carcinomas. Cancer Res 2007; 67: 11601–11.
34. Takano A, Ishikawa N, Nishino R, Masuda K, Yasui W, Inai K, et al. Identification of nectin-4 oncoprotein as a diagnostic and therapeutic target for lung cancer. Cancer Res 2009; 69: 6694–703.
35. Sato N, Yamabuki T, Takano A, Koinuma J, Aragaki M, Masuda K, et al. Wnt inhibitor Dickkopf-1 as a target for passive cancer immunotherapy. Cancer Res 2010; 70: 5326–36.
36. Aragaki M, Takahashi K, Akiyama H, Tsuchiya E, Kondo S, Nakamura Y, et al. Characterization of a cleavage stimulation factor, 3' pre-RNA, subunit 2, 64 kDa (CSTF2) as a therapeutic target for lung cancer. Clin Cancer Res 2011; 17: 5889–900.
37. Nishino R, Takano A, Oshita H, Ishikawa N, Akiyama H, Ito H, et al. Identification of Epstein-Barr virus-induced gene 3 as a novel serum and tissue biomarker and a therapeutic target for lung cancer. Clin Cancer Res 2011; 17: 6272–86.
38. Masuda K, Takano A, Oshita H, Akiyama H, Tsuchiya E, Kohno N, et al. Chondrolectin is a novel diagnostic biomarker and a therapeutic target for lung cancer. Clin Cancer Res 2011; 17: 7712–22.
39. Fujitomo T, Daigo Y, Matsuda K, Ueda K, Nakamura Y. Critical Function for Nuclear Envelope Protein TMEM209 in Human Pulmonary Carcinogenesis. Cancer Res 2012; 72: 4110–8.
40. Koinuma J, Akiyama H, Fujita M, Hosokawa M, Tsuchiya E, Kondo S, et al.. Characterization of an Opa interacting protein 5 involved in lung and esophageal carcinogenesis. Cancer Sci 2012; 103: 577–86.
41. Nguyen MH, Ueda K, Nakamura Y, Daigo Y. Identification of a novel oncogene, MMS22L, involved in lung and esophageal carcinogenesis. Int J Oncol 2012 in press.

42. Shintani M, Tada M, Kobayashi T, Kajiho H, Kontani K, Katada T. Characterization of Rab45/RASEF containing EF-hand domain and a coiled-coil motif as a self-associating GTPase. Biochem Biophys Res Commun 2007;357:661–7.
43. Sobin L, Wittekind Ch. TNM classification of malignant tumours. 6th ed. New York: Wiley-Liss;2002.
44. Bhuin T, Roy JK. *Rab11* regulates JNK and Raf/MAPK-ERK signalling pathways during *Drosophila* wing development. Cell Biology International 2010;34:1113–8.
45. Montalbano J, Lui K, Sheikh MS, Huang Y. Identification and characterization of RBEL1 subfamily of GTPases in the Ras superfamily involved in cell growth regulation. J Biol Chem 2009;284:18129–42.
46. Chang F, Steelman LS, Lee JT, Shelton JG, Navolanic PM, Blalock WL, et al. Signal transduction mediated by the Ras/Raf/MEK/ERK pathway from cytokine receptors to transcription factors: potentialtargeting for therapeutic intervention. Leukemia 2003;17:1263–93.
47. Jürchott K, Kuban RJ, Krech T, Blüthgen N, Stein U, Walther W, et al. Identification of Y-box binding protein 1 as a core regulator of MEK/ERK pathway-dependent gene signatures in colorectalcancer cells. PLoS Genet 2010;6:e1001231.
48. Maat W, Beiboer SH, Jager MJ, Luyten GP, Gruis NA, van der Velden PA. Epigenetic regulation identifies RASEF as a tumor-suppressor gene in uveal melanoma. Invest Ophthalmol Vis Sci 2008;49:1291–8.
49. Zhang X, Lin P, Zhu ZH, Long H, Wen J, Yang H, et al. Expression profiles of early esophageal squamous cell carcinoma by cDNA microarray. Cancer Genet Cytogenet 2009;194:23–9.
50. Friday BB, Adjei AA. Advances in targeting the Ras/Raf/MEK/Erk mitogen-activated protein kinase cascade with MEK inhibitors for cancer therapy. Clin Cancer Res 2008;14:342–6.

Figure legends

Figure 1. RASEF expression in tumor tissues and cell lines.

A, Expression of *RASEF* in 12 clinical lung cancers [T; 4 clinical lung adenocarcinomas (ADC), 4 clinical lung squamous cell carcinomas (SCC) and 4 clinical small cell lung cancers (SCLC)] and corresponding normal lung tissues (N) detected by semiquantitative RT-PCR analysis. ***B,*** Expression of *RASEF* in 22 lung cancer cell lines and a bronchial epithelial cell line BEAS-2B detected by semiquantitative RT-PCR analysis. ASC indicates lung adenosquamous cell carcinoma; LCC, large cell carcinoma. ***C*****,** Western blot analysis of RASEF protein using anti-RASEF antibody. IB, immunoblotting. ***D*****,** Expression and subcellular localization of endogenous RASEF protein in RASEF-positive and -negative lung cancer cell lines, and bronchial epithelial cells. RASEF was stained mainly at the cytoplasm in A549 and NCI-H2170 cells, whereas no staining was observed in DMS114 and bronchial epithelia derived BEAS-2B cell lines.

Figure 2. RASEF expression in tumor tissues and normal tissues.

A**,** Northern blot analysis of the *RASEF* transcript in 16 normal adult human tissues. A weak signal was observed in only prostate and testis. ***B*****,** Expression of RASEF protein expression between normal tissues and lung cancers by immunohistochemistry. Original magnification, X200. ***C*****,** Immunohistochemistry of lung tumor tissues and adjacent normal lung tissues. Original magnification, X100. ***D*****, *E*****,** Prognostic significance of high RASEF expression in surgically treated non-small cell lung cancer (NSCLC) patients evaluated by tissue microarray. Examples for strong, weak, and absent RASEF expression in lung cancer tissues and a normal tissue (***D***). Original magnification, x100. Kaplan-Meier analysis of tumor-specific survival of NSCLC patients (n = 341) who underwent resection of primary tumors according to expression levels of RASEF ($P < 0.0001$ by log-rank test) (***E***). Makers on survival curves mean censored cases.

Figure 3. Growth promoting effect of RASEF.

A-C, Inhibition of growth of lung cancer cells by siRNAs against RASEF. Knockdown of RASEF protein expression in A549 and NCI-H2170 cells transfected with si-RASEFs (#1 and #2) and control siRNAs (si-EGFP and si-LUC), analyzed by Western blotting (***A***). Cell viability and colony numbers detected by MTT assay (***B***) and Colony formation assay (***C***). ***D, E,*** Growth promotion of BEAS-2B and DMS114 cells by overexpression of exogenous RASEF. Detection of transient RASEF expression by Western blot analysis with anti-Flag antibody (***D***). MTT assays of BEAS-2B and DMS114 cells 120 hours after transfection of RASEF-expressing vector (***E***). Columns, relative absorbance of triplicate assays; bars, SD.

Figure 4. Enhanced phosphorylation of ERK1/2 by RASEF in lung cancer cells.
A, Expression of MAPK signal molecules and their phosphorylation levels in DMS114 cells transfected with RASEF-expression vector or mock plasmid. ***B,*** Expression of MAPK signal molecules and their phosphorylation levels in NCI-H2170 cells transfected with siRNAs for RASEF (si-RASEF#2) or control siRNAs (si-LUC). ***C, D,*** Expression levels of downstream target genes of MAPK cascade were regulated by RASEF expression in lung cancer cells. Total RNA from BEAS-2B and DMS114 cells transfected with RASEF-expression vector or mock plasmid (***C***) and A549 and NCI-H2170 cells transfected with siRNAs for RASEF (si-RASEF#2) or control siRNAs (si-LUC) (***D***) were subjected to reverse-transcription reaction, followed by PCR reaction to evaluate the expression levels of *CCND1, CCNB1,* and *CDKN1A* transcription. Western blotting with anti-phosphorylated ERK1/2 antibody was performed to confirm the change of ERK1/2 phosphorylation according to RASEF expression.

Figure 5. Identification of ERK1/2-interacting sites on RASEF.
A, Interaction of endogenous RASEF with endogenous ERK1/2. The immunoprecipitates obtained using anti-RASEF antibody were subjected to Western blotting with anti-ERK1/2 antibody. ***B,*** Schematic representation of various partial constructs of RASEF expression vector. ***C, D,*** Determination of the ERK1/2-interacting regions on RASEF by immunoprecipitation experiments

using DMS114 cells transfected with vectors expressing partial RASEF protein. COOH-terminal part of RASEF (codons 520-575) was likely to be ERK1/2-interacting region.

Figure 6. Growth inhibition of lung cancer cells by dominant-negative peptides inhibiting RASEF-ERK1/2 interaction.

A, Schematic drawing of three cell-permeable peptides of RASEF covering codons 520-575 of RASEF that corresponds to the ERK-interacting region. ***B, C,*** Growth suppressive effect of dominant-negative peptides on lung cancer cells. 11R-RASEF$_{553\text{-}575}$ peptides showed dose-dependent growth suppressive effect on RASEF-positive cells. Columns, relative absorbance of triplicate MTT assays; bars, SD; *, $P < 0.05$; **, $P < 0.0001$; N.S., Not significant. ***D,*** Inhibition of binding between endogenous RASEF and ERK1/2 using cell-permeable peptide, detected by immunoprecipitation assay. NCI-H2170 cells were lysed after treatment either with 11R-RASEF$_{553\text{-}575}$ peptides or with scramble peptide for 4 hours. The immunoprecipitates with anti-RASEF antibody were subjected to Western blotting with anti-ERK1/2 antibody.

Author Manuscript Published OnlineFirst on May 16, 2013; DOI: 10.1158/1541-7786.MCR-12-0685-T
Author manuscripts have been peer reviewed and accepted for publication but have not yet been edited.

Table 1A. Association between RASEF-positivity in NSCLC tissues and patients' characteristics (n=341)

		RASEF expression			*P* value
	Total	Strong expression	Weak expression	Absent expression	strong vs weak or absent
	n=341	n=126	n=150	n=65	
Gender					
Female	100	33	47	20	0.3885
Male	241	93	103	45	
Age(year)					
< 65	160	59	70	31	0.9999
>=65	181	67	80	34	
Smoking status					
never smoker	93	33	39	21	0.8014
current or ex-smoker	248	93	111	44	
Histological type					
ADC	205	68	96	41	0.1094
non-ADC	136	58	54	24	
T factor					
T1	141	37	68	36	0.0006*
T2+T3	200	89	82	29	
N factor					
N0	223	74	100	49	0.0590
N1+N2	118	52	50	16	

**P* < 0.05 (Fisher's exact test)

ADC, adenocarcinoma

non-ADC, squamouse cell carcinoma plus large cell carcinoma and adenosquamous cell carcinoma

Table 1B. Cox's proportional hazards model analysis of prognostic factors in patients with NSCLCs

Variables	Hazards ratio	95% CI	Unfavorable/Favorable	*P*-value
Univariate analysis				
RASEF	2.065	1.458-2.927	strong positive / weak positive or absent	<0.0001*
Age (years)	1.488	1.042-2.125	>= 65 / 65 >	0.0287*
Gender	1.612	1.065-2.441	Male / Female	0.0239*
Smoking status	1.288	0.855-1.941	Current or ex-smoker / never smoker	0.2252
Histological type	1.427	1.007-2.023	non-ADC/ADC	0.0455*
pT factor	2.824	1.874-4.255	T2+T3 / T1	<0.0001*
pN factor	2.538	1.791-3.596	N1+N2 / N0	<0.0001*
Multivariate analysis				
RASEF	1.697	1.191-2.418	strong positive / weak positive or absent	0.0034*
Age (years)	1.663	1.158-2.389	>= 65 / 65 >	0.0058*
Gender	1.299	0.822-2.054	Male / Female	0.2620
Histological type	0.902	0.612-1.330	non-ADC/ADC	0.6033
pT factor	2.171	1.403-3.361	T2+T3 / T1	0.0005*
pN factor	2.200	1.532-3.158	N1+N2 / N0	<0.0001*

ADC, adenocarcinoma

non-ADC, squamous-cell carcinoma plus large-cell carcinoma and adenosquamous-cell carcinoma

*$P < 0.05$

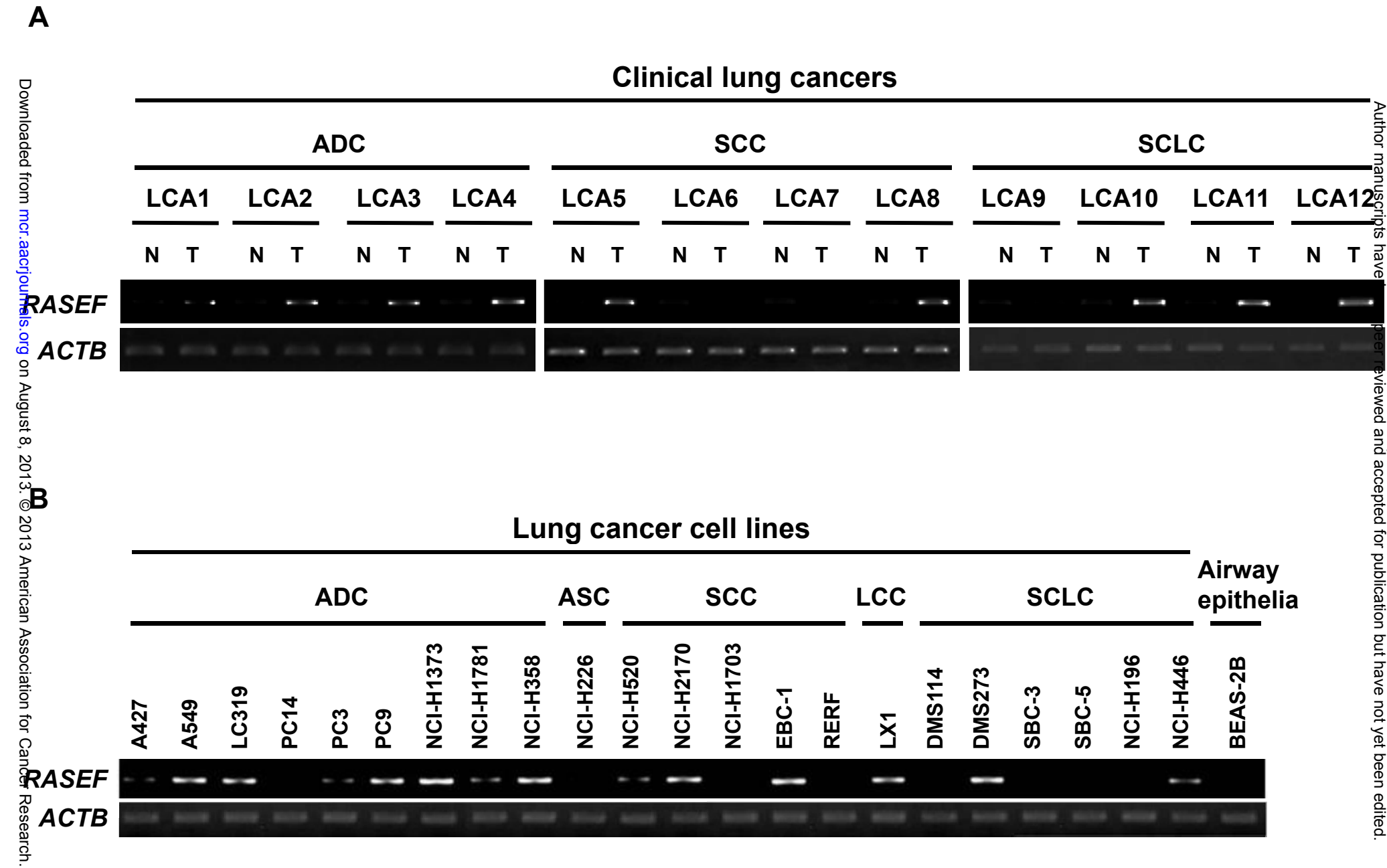

Fig. 1

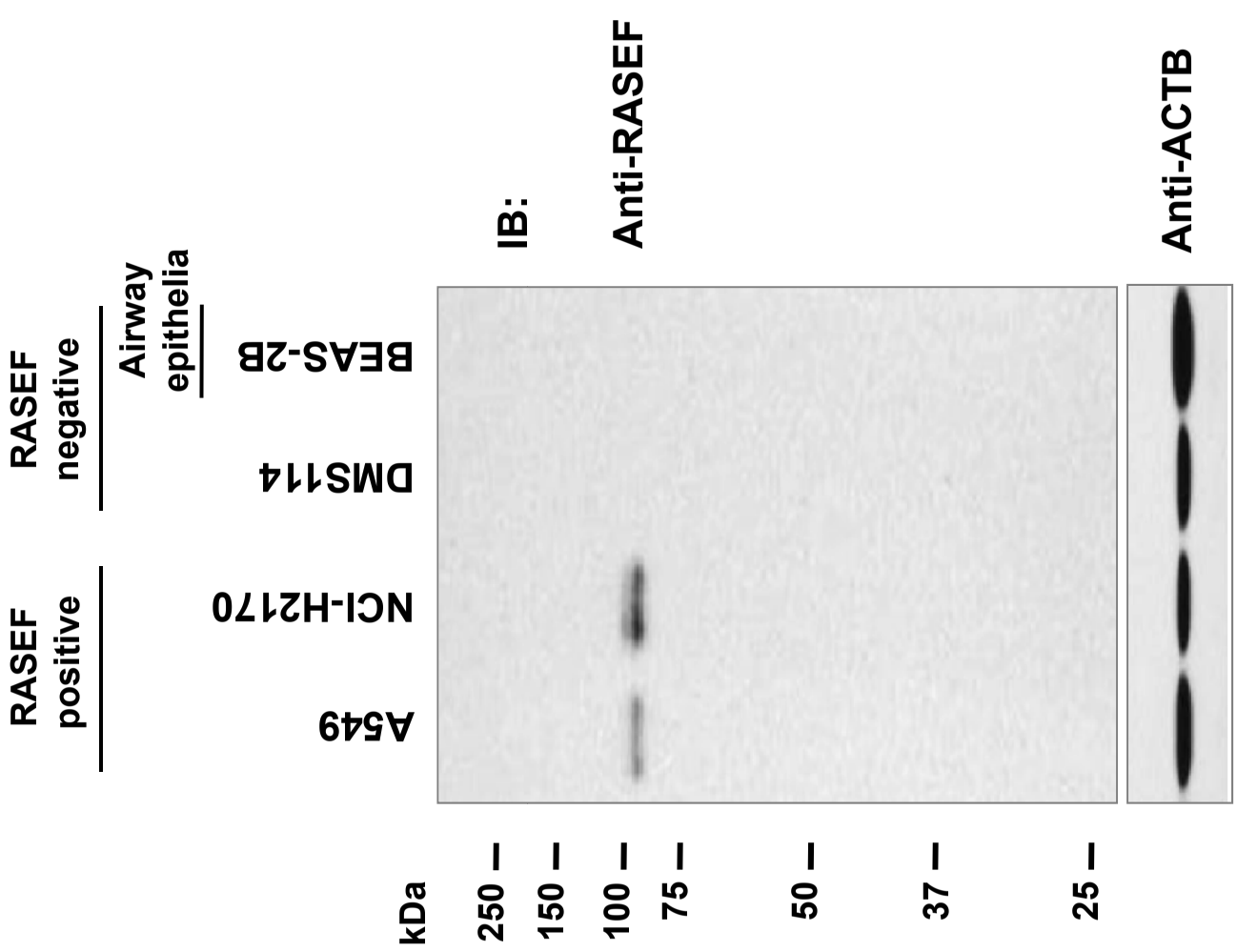

Fig. 1

C

D

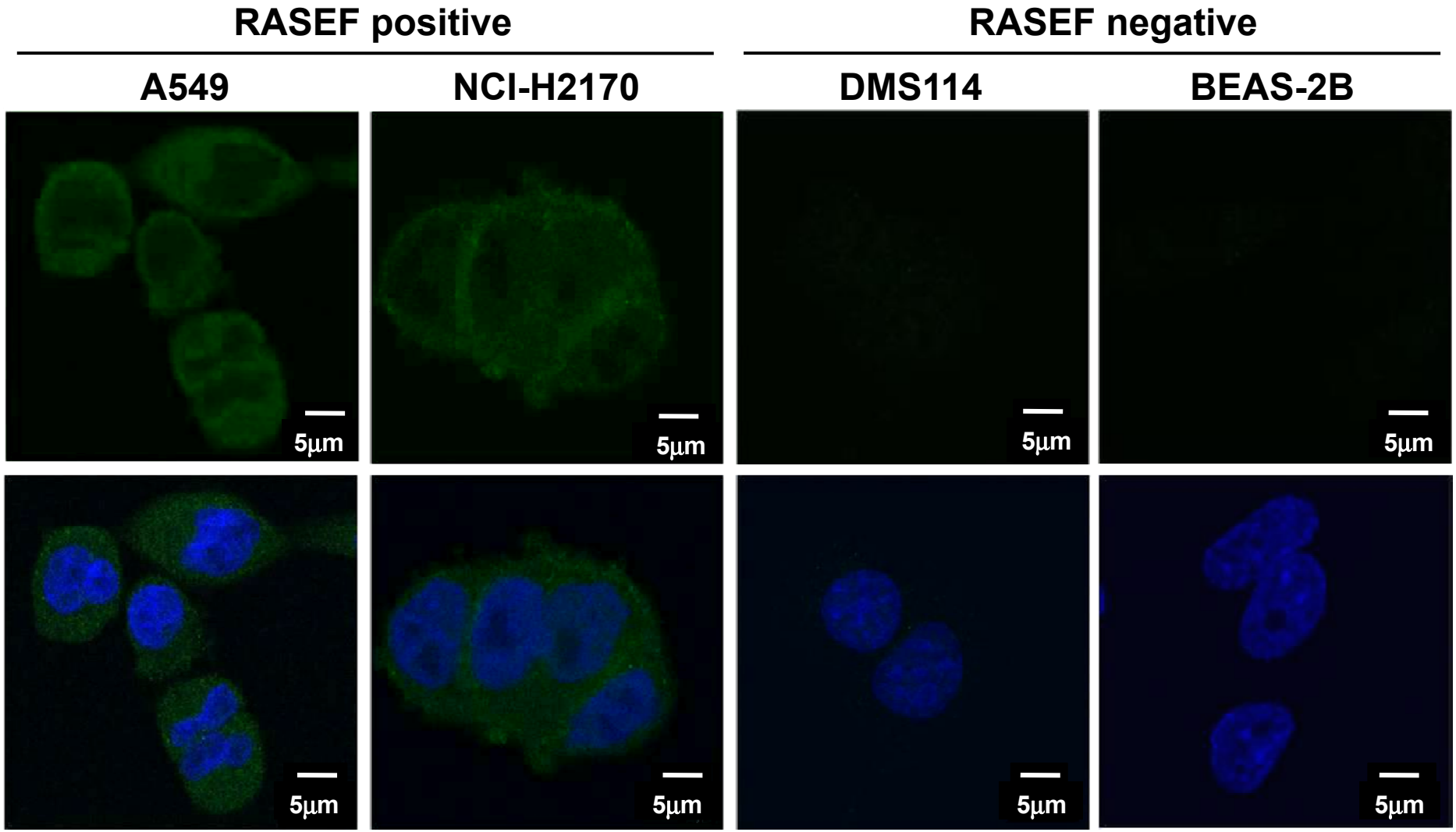

Fig. 1

Author Manuscript Published OnlineFirst on May 16, 2013; DOI: 10.1158/1541-7786.MCR-12-0685-T
Author manuscripts have been peer reviewed and accepted for publication but have not yet been edited.

Fig. 2

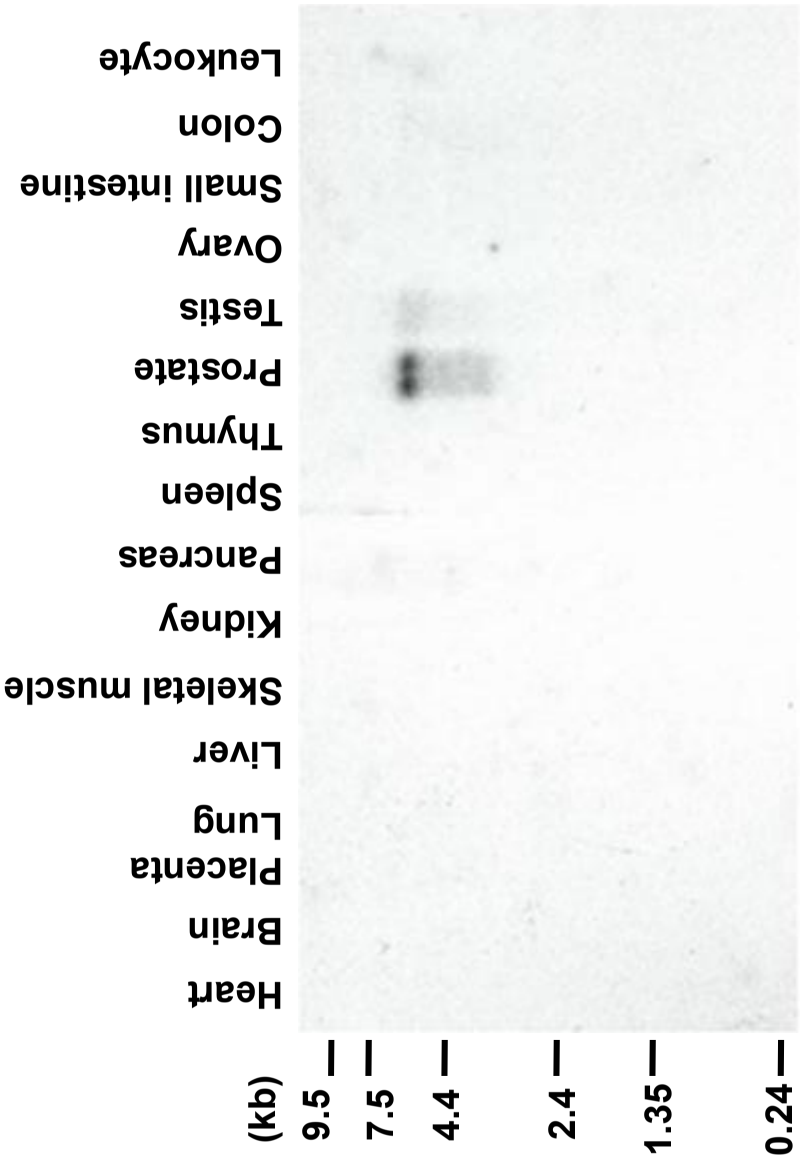

A

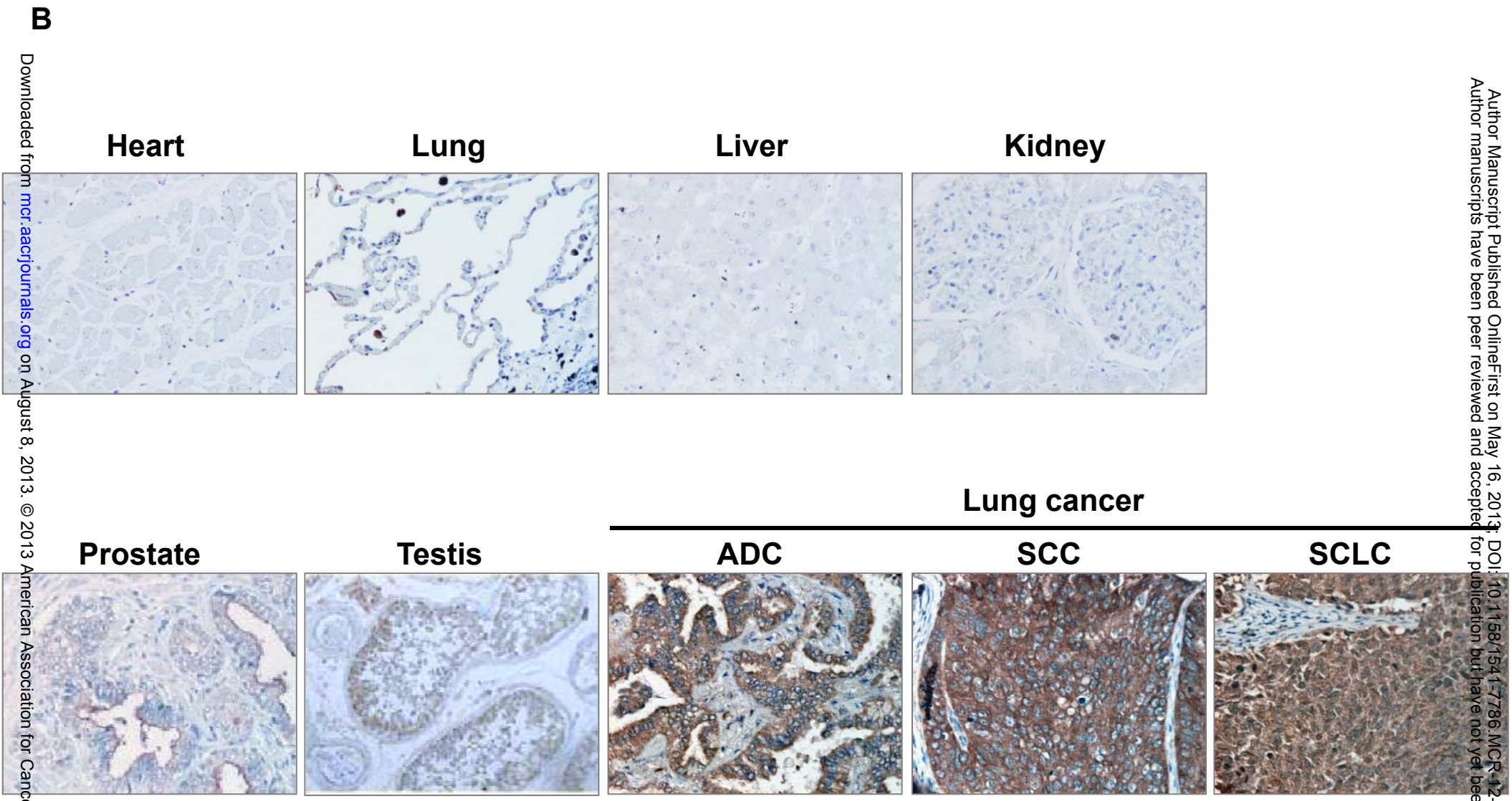

Fig. 2

Author Manuscript Published OnlineFirst on May 16, 2013; DOI: 10.1158/1541-7786.MCR-12-0685-T
Author manuscripts have been peer reviewed and accepted for publication but have not yet been edited.

Fig. 2

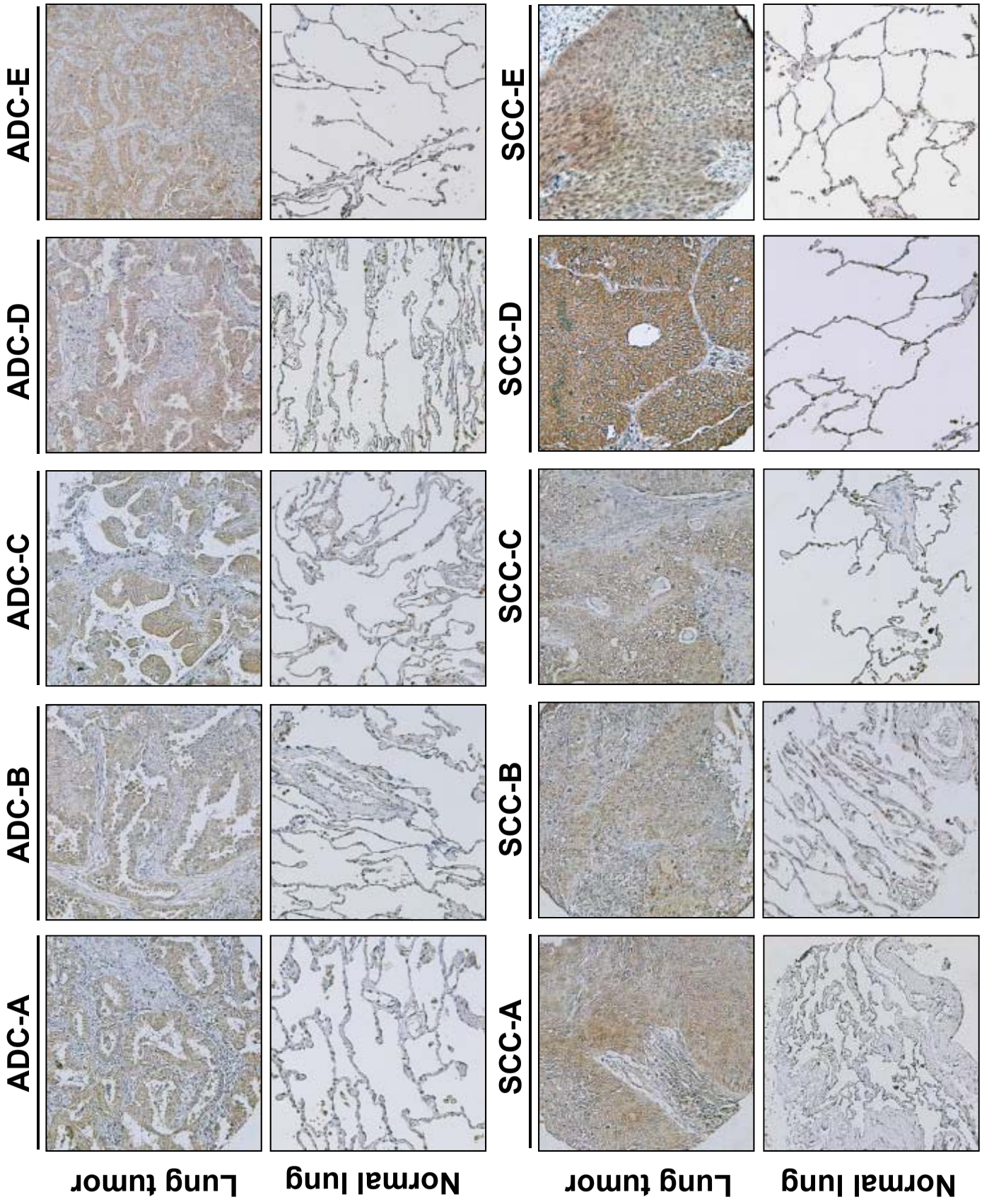

C

D

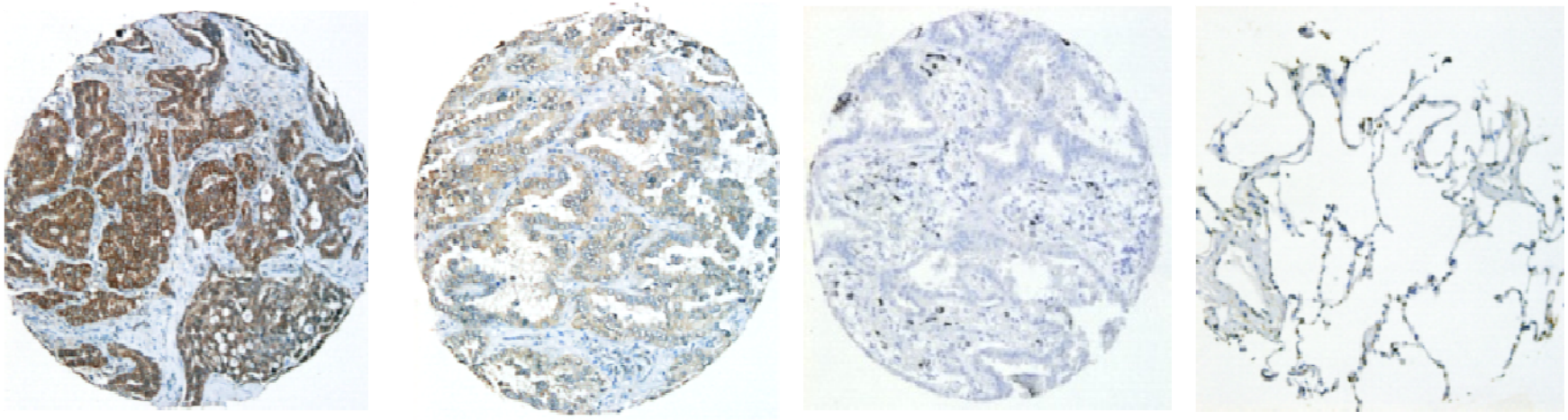

E

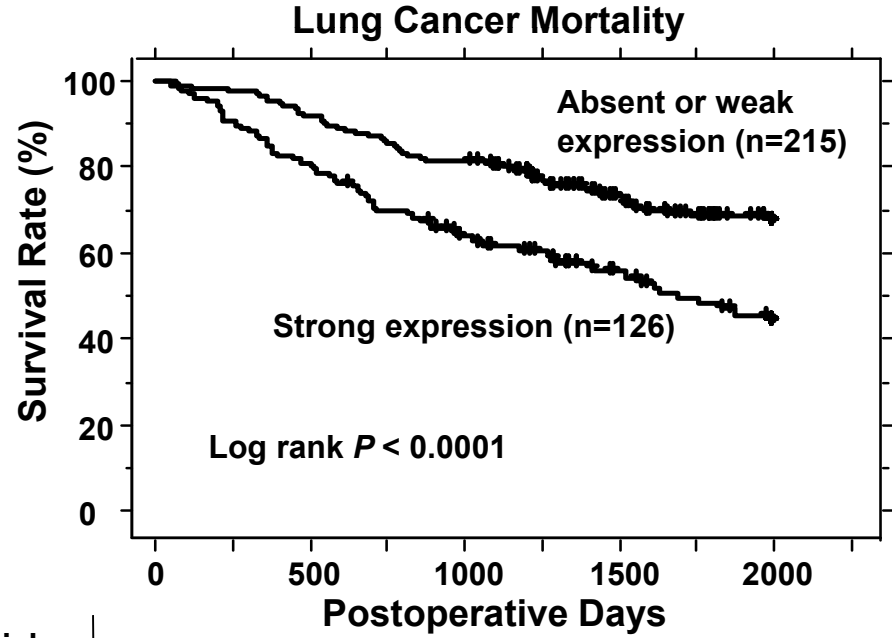

Number of patients at risk	0	500	1000	1500	2000
Absent or weak RASEF expression	215	198	175	120	81
Strong RASEF expression	126	102	75	47	33

Fig. 2

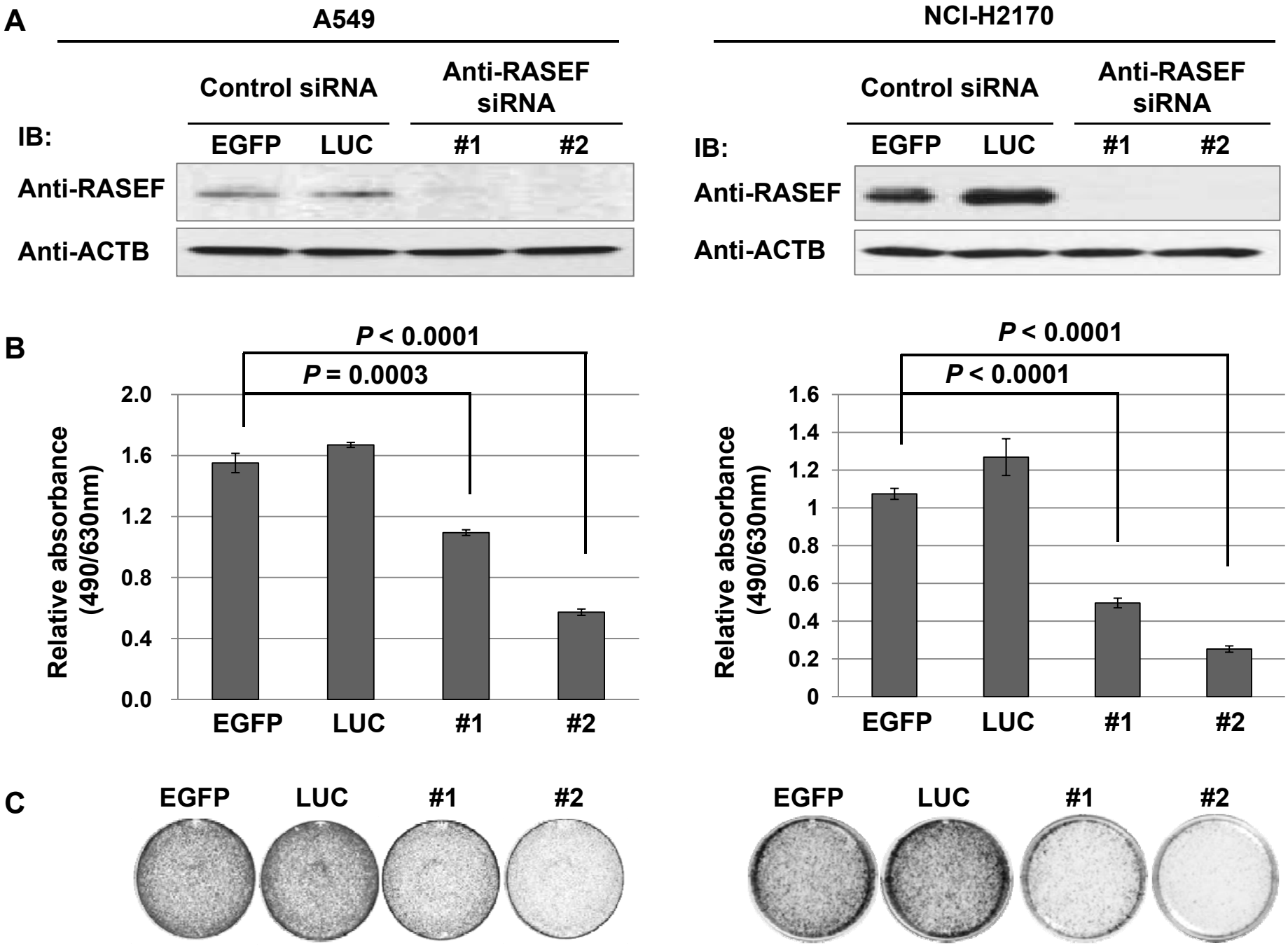

Fig. 3

D

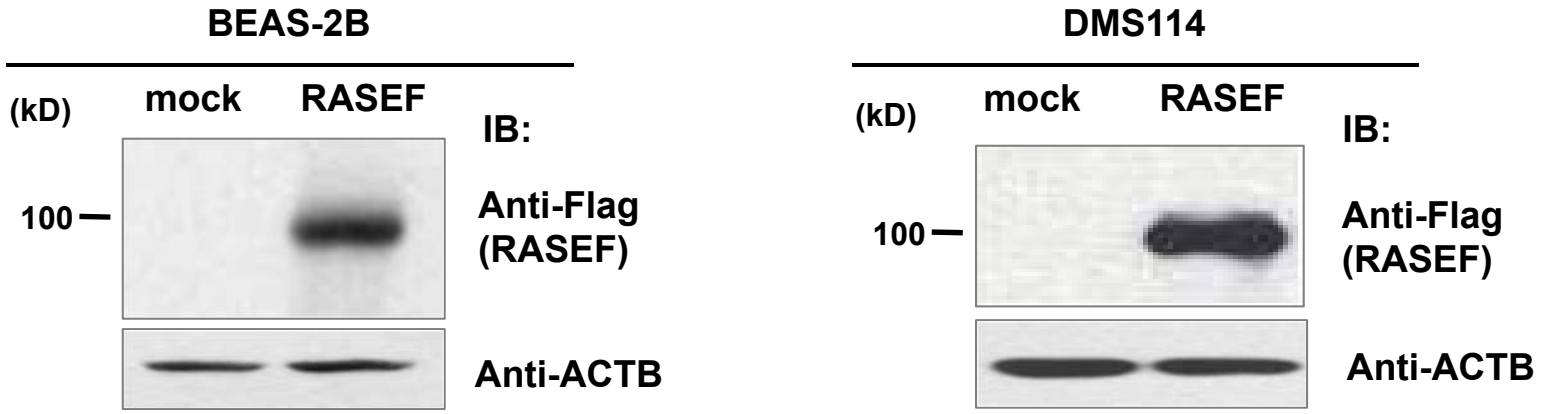

E

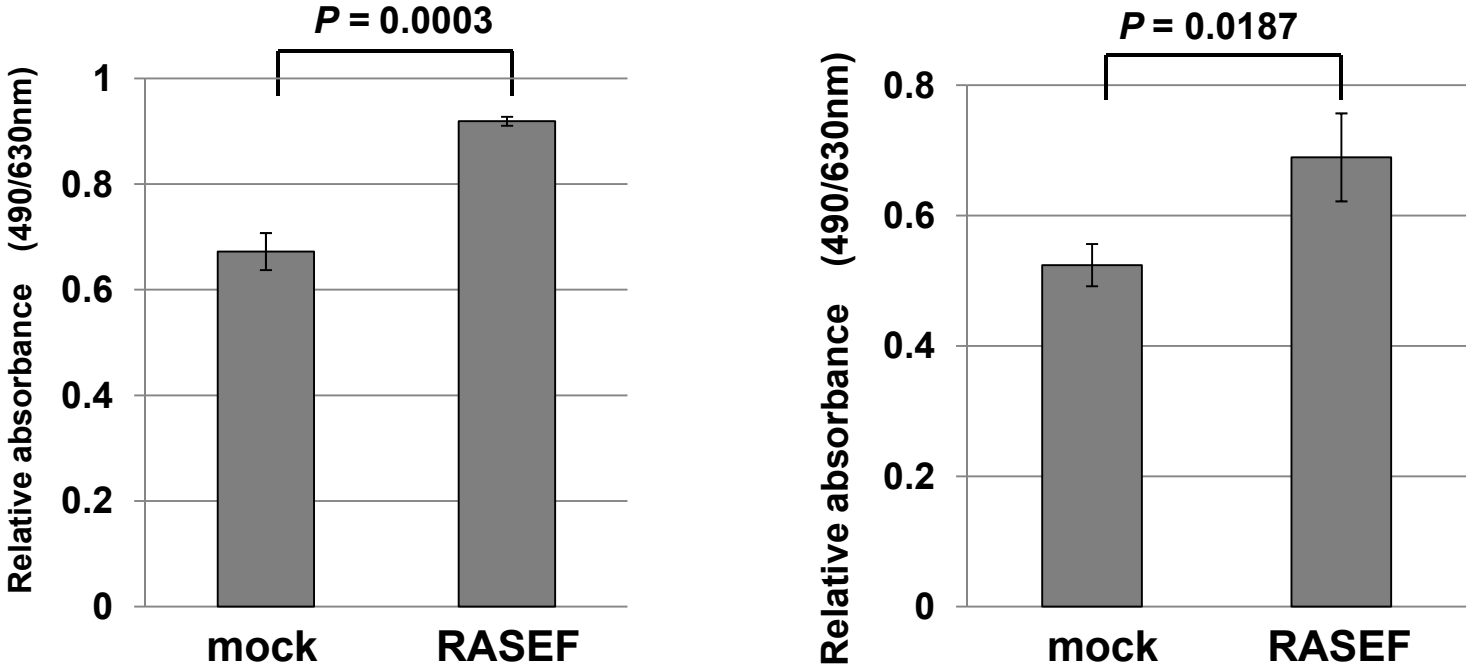

Fig. 3

Author Manuscript Published OnlineFirst on May 16, 2013; DOI: 10.1158/1541-7786.MCR-12-0685-T
Author manuscripts have been peer reviewed and accepted for publication but have not yet been edited.

Fig. 4

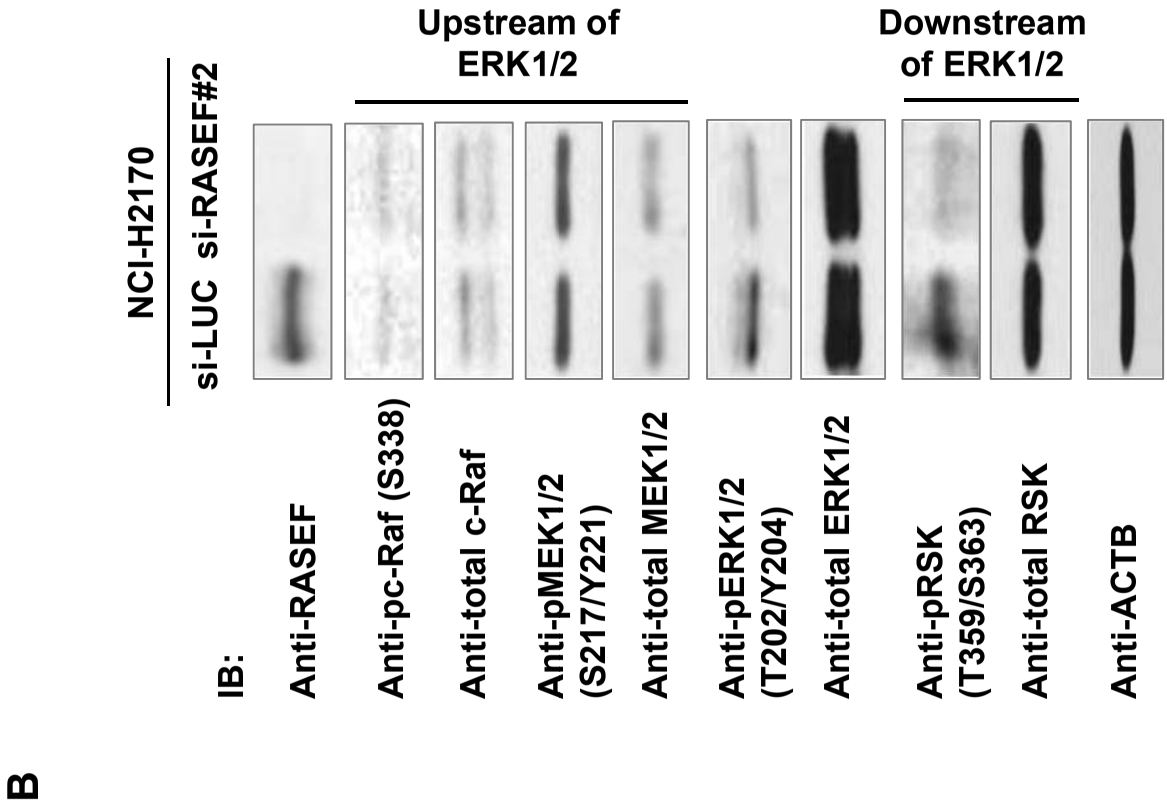

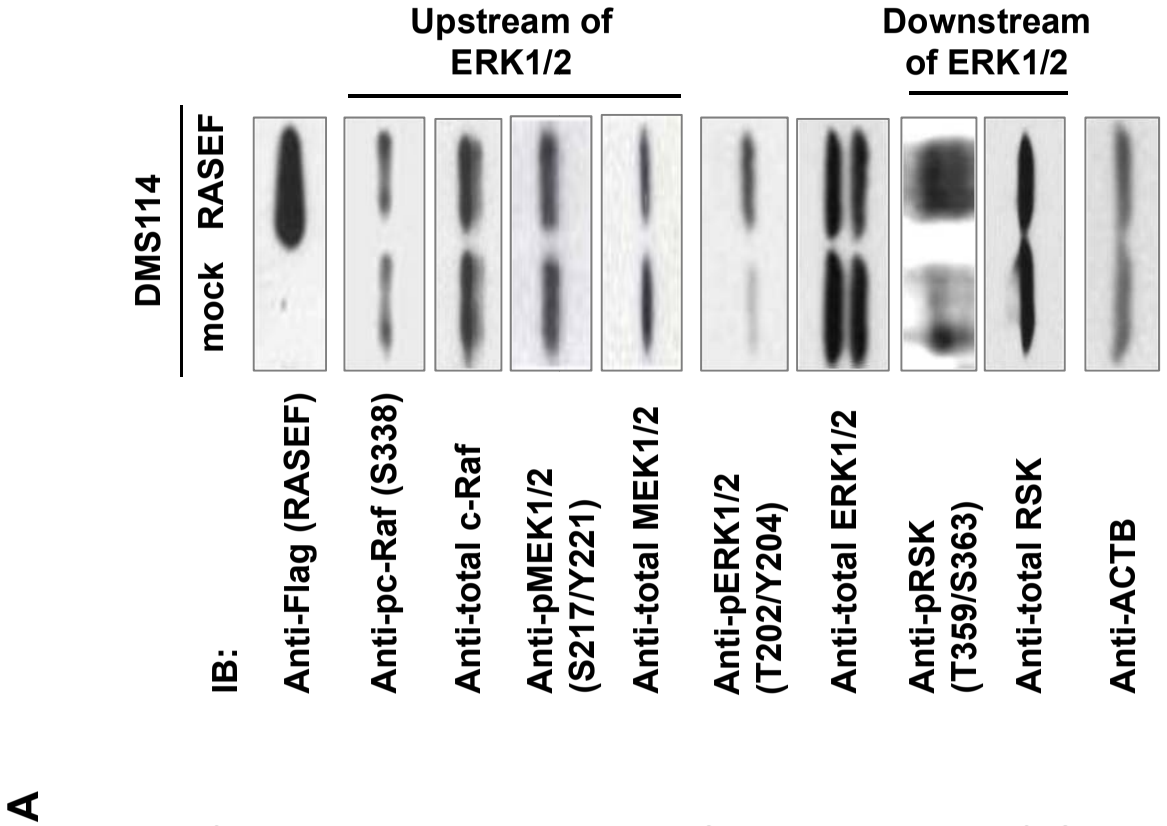

Fig. 4

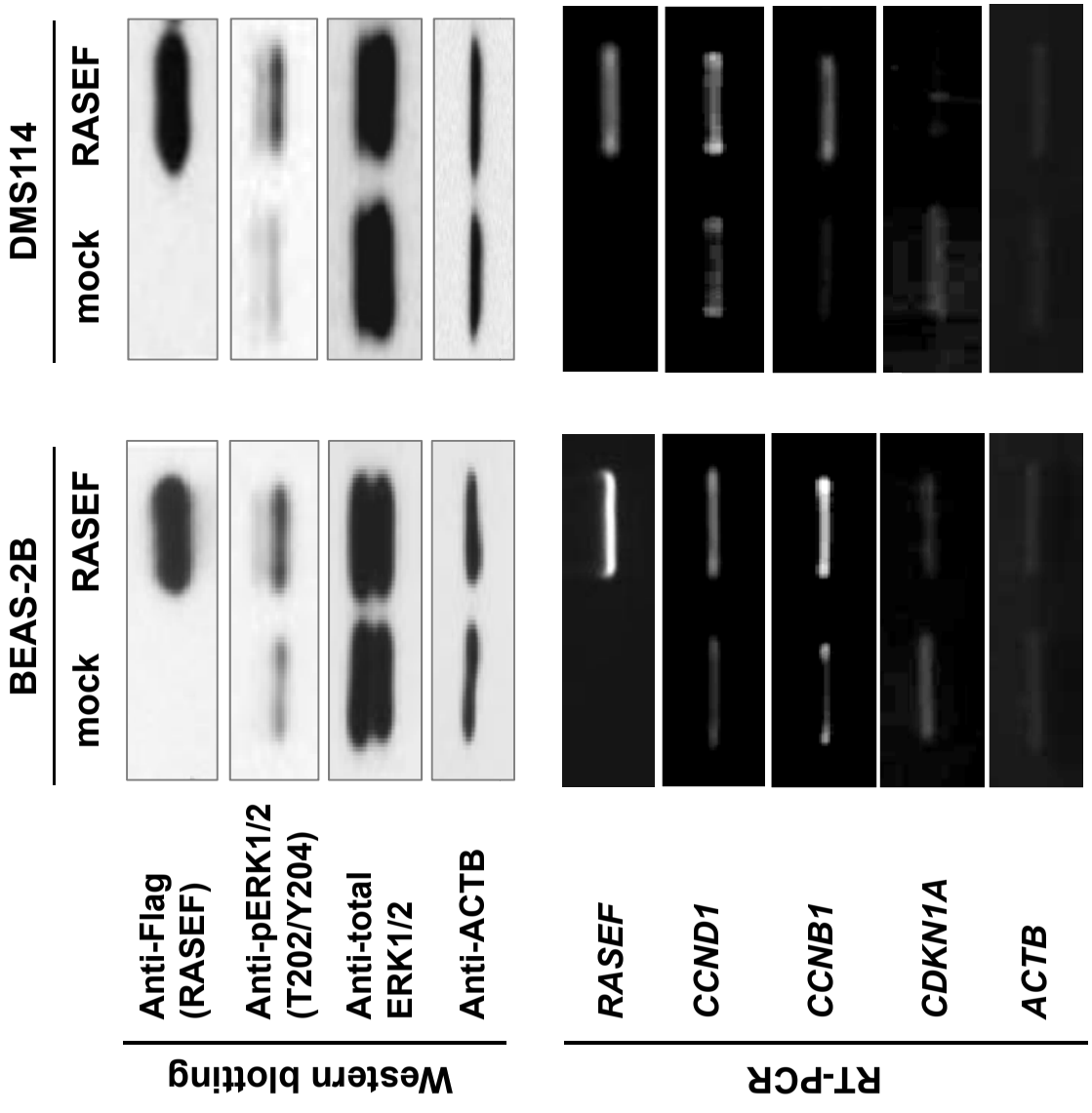

C

Fig. 4

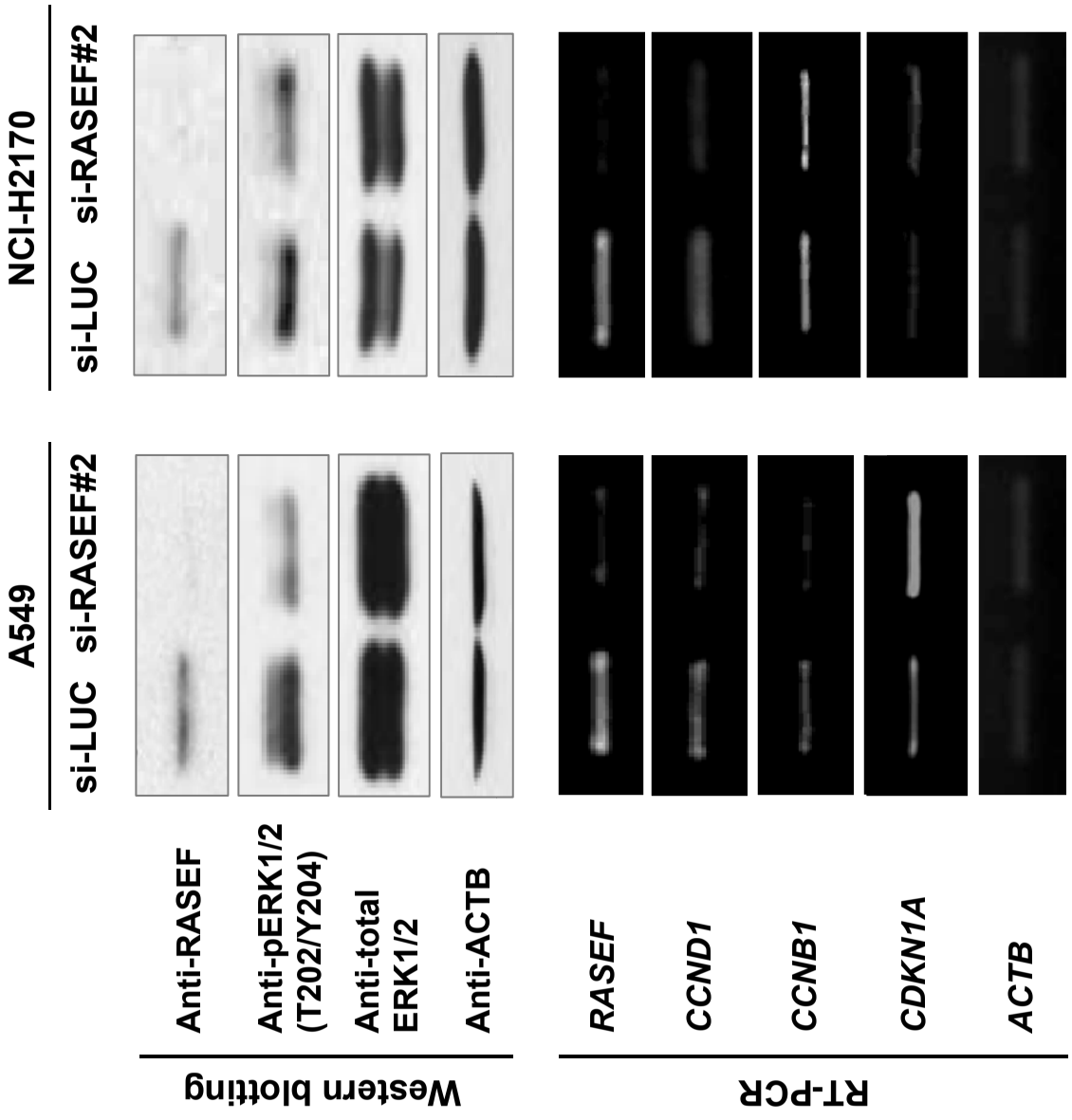

D

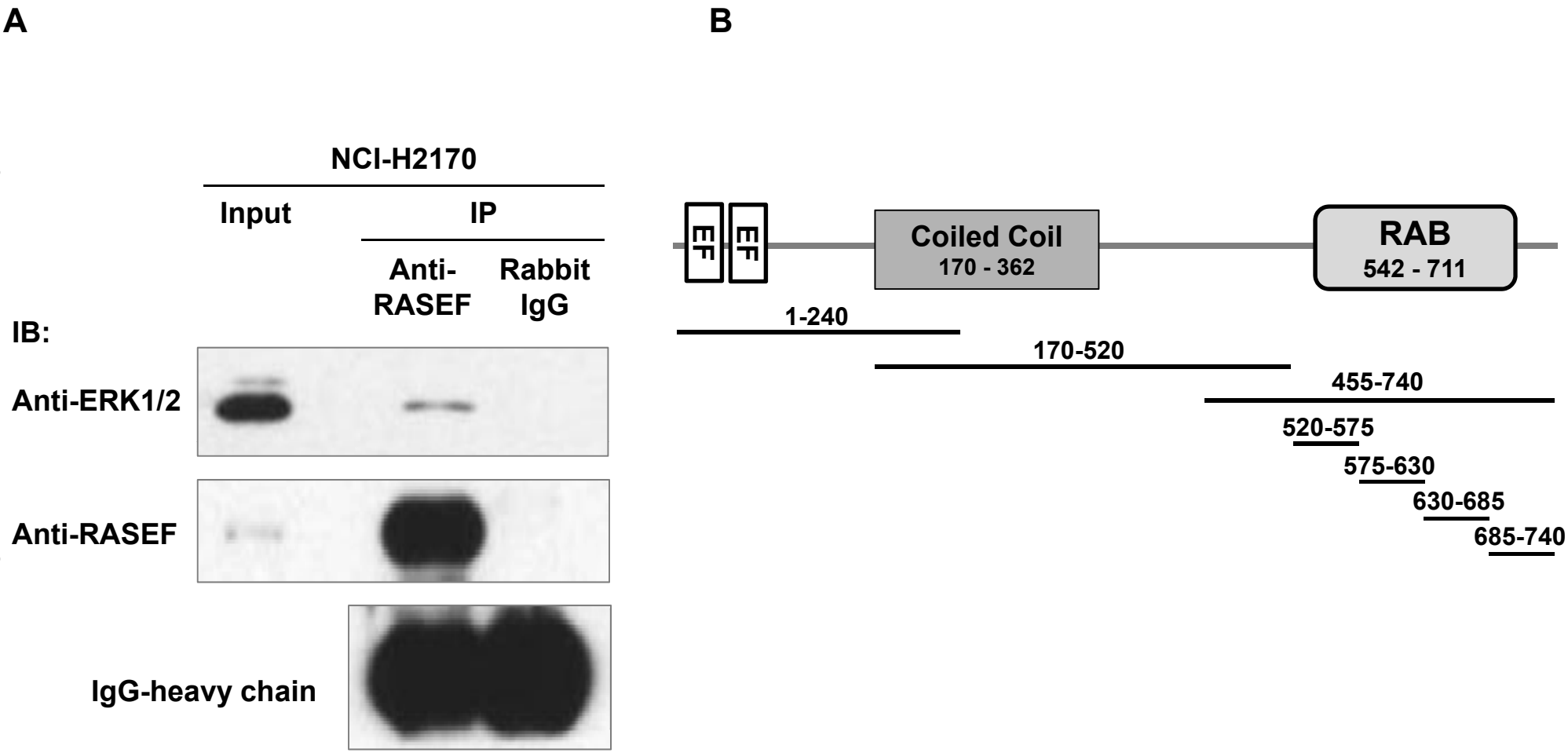

Fig. 5

Fig. 5

A

Fig. 6

B

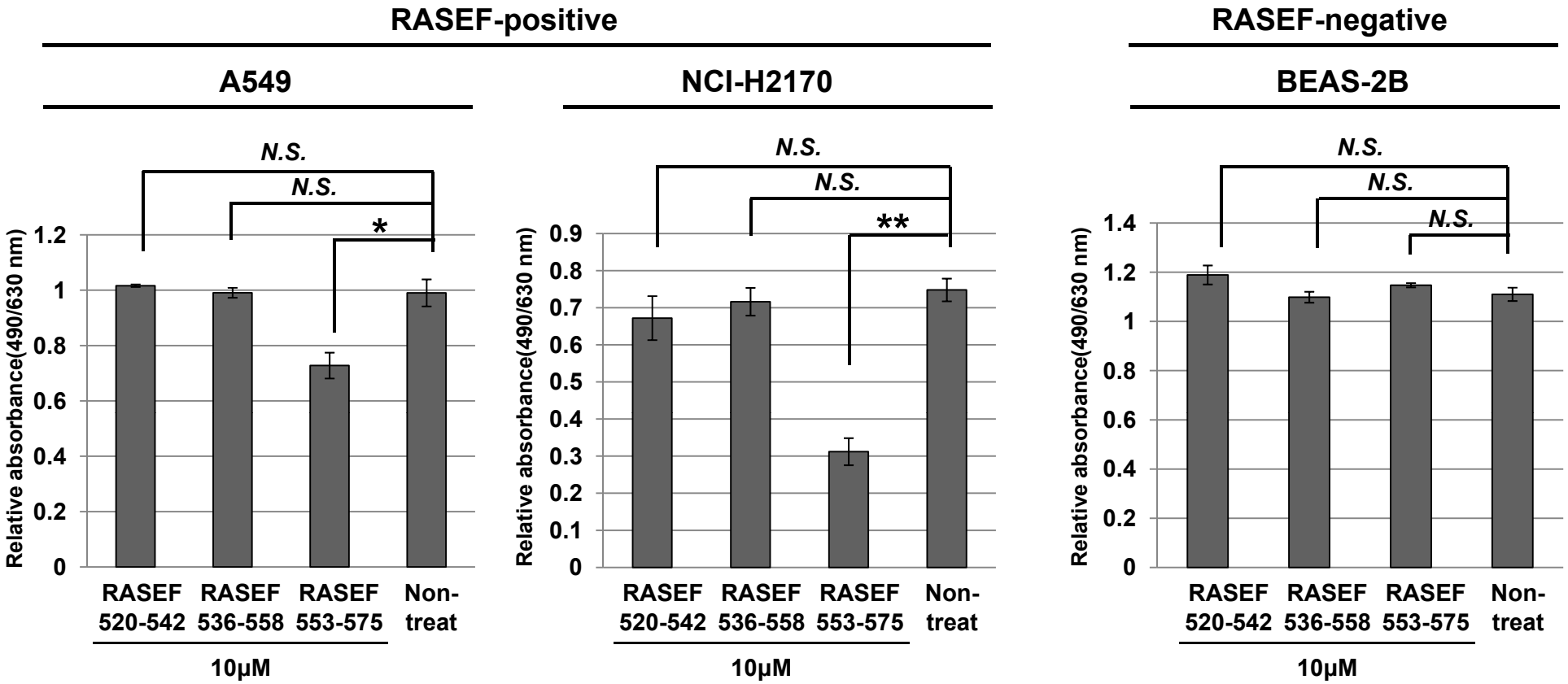

Fig. 6

C

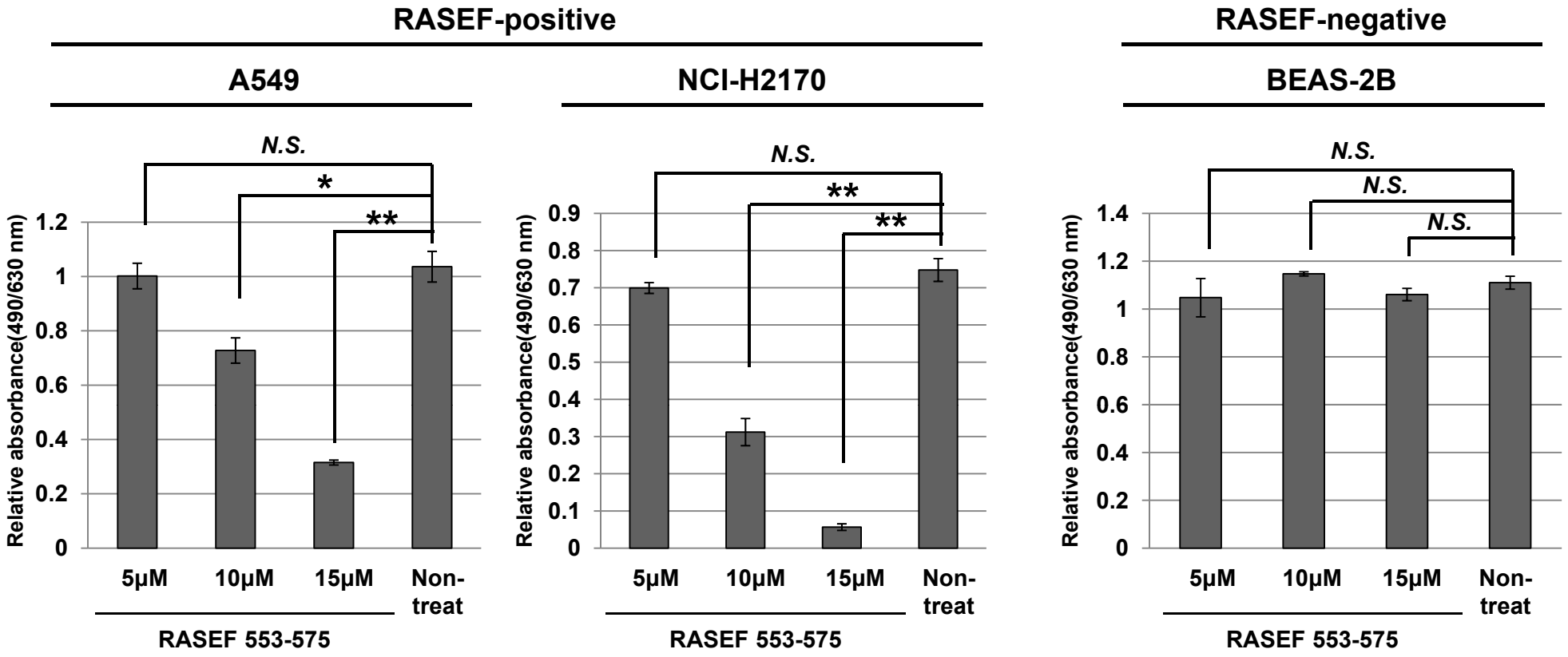

Fig. 6

D

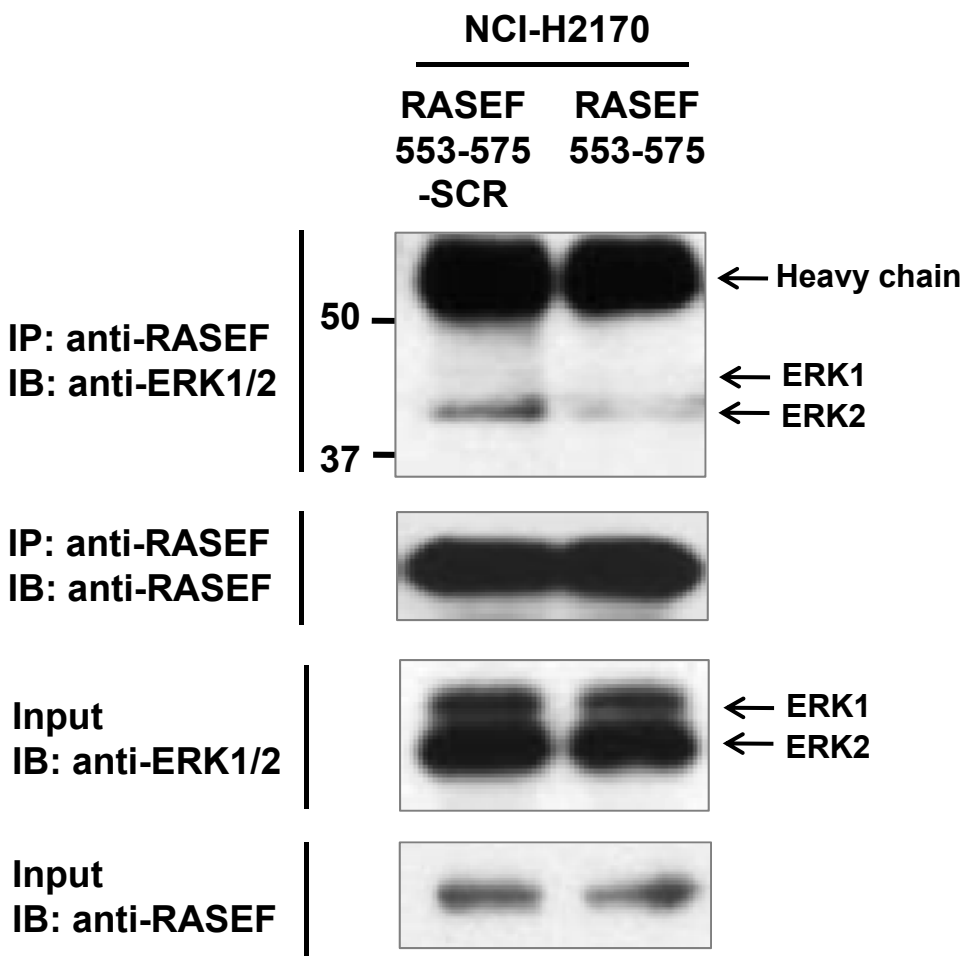

Fig. 6